

We are IntechOpen, the world's leading publisher of Open Access books Built by scientists, for scientists

6,900

Open access books available

186,000

International authors and editors

200M

Downloads

Our authors are among the

154

Countries delivered to

TOP 1%

most cited scientists

12.2%

Contributors from top 500 universities



WEB OF SCIENCE™

Selection of our books indexed in the Book Citation Index
in Web of Science™ Core Collection (BKCI)

Interested in publishing with us?
Contact book.department@intechopen.com

Numbers displayed above are based on latest data collected.
For more information visit www.intechopen.com



Ocean Wind Energy Technologies in Modern Electric Networks: Opportunity and Challenges

*Foad H. Gandoman, Abdollah Ahmadi,
Shady H.E. Abdel Aleem, Masoud Ardehshiri,
Ali Esmaeel Nezhad, Joeri Van Mierlo and Maitane Berecibar*

Abstract

Wind energy is one of the most important sources of energy in the world. In recent decades, wind as one of the massive marine energy resources in the ocean to produce electricity has been used. This chapter introduces a comprehensive overview of the efficient ocean wind energy technologies, and the global wind energies in both offshore and onshore sides are discussed. Also, the classification of global ocean wind energy resources is presented. Moreover, different components of a wind farm offshore as well as the technologies used in them are investigated. Possible layouts regarding the foundation of an offshore wind turbine, floating offshore, as well as the operation of wind farms in the shallow and deep location of the ocean are studied. Finally, the offshore wind power plant challenges are described.

Keywords: ocean wind energy, offshore wind energy conversion, offshore renewable energy, power transmission, offshore wind turbines, active and reactive powers

1. Ocean wind energy resource

The increasing demand for electric power, the limited availability of fossil fuels, and increased environmental pollution have made it essential to Integra Clean Energy sources such as wind in our energy systems. On the other hand, the shortage of drought and varieties of geographical possibilities justifies the approach to developing offshore wind farms.

The offshore wind farms are wind turbines that are built several kilometers offshore in the ocean or sea for more efficient utilization of wind energy. Although this method is already very costly, increasing technological advances in turbines materials and bases, composite structures, as well as the construction of multimegawatt generators accelerate the deployment of offshore wind farms and make them a huge part of future energy production [1–3].

This chapter starts with introduction to the wind energy resource. After that, the global ocean wind energy resource is presented. Ocean wind energy technologies

are explained in the next section. Then, the possible structure of offshore wind turbine is considered. Finally, challenges of offshore wind power are discoursed.

One of the renewable energy resources that can be used to generate electricity is ocean wind. Two-thirds of the Earth's surface is water; this potential could be used to generate electricity in different parts of the planet. However, using the ocean wind source varies depending on the geographical conditions and seasons. Currently, the UK has the world's leading outsourcing of 51% of its offshore power plants. Denmark with 21% of the total offshore power plants in the world is in the second place. Other countries such as the USA, the Netherlands, Belgium, China, and Japan are also active in this field [4]. **Figure 1** shows the items that need to be considered in the market for the production and sale of electricity through ocean wind energy. The most critical issues regarding the wind ocean project are foundation type and water depth which are based on geographic information in the region.

1.1 Global ocean wind energy resource

1.1.1 Ocean wind energy in Asia

Over the past few decades, large countries like China and Japan have been using ocean wind energy for electricity production. According to wind energy reports at the World Wind Energy Council, China's investment in this area is more than the total European Union and is about 3.4 GW [5].

East Asia has a high potential for exploiting ocean wind energy, and many projects in this area, specifically in China, South Korea, and Japan, have been carried out and implemented. Among Asian countries, China has more shares in the use of wind energy. China was the first country in the Asia-Pacific region which used wind ocean energy. **Table 1** shows several offshore wind energy projects in Asia [5, 6].

China had installed more than 3.4 GW of ocean wind capacity at the end of 2016 and should end up with around 900 GW more by the end of 2030. According to

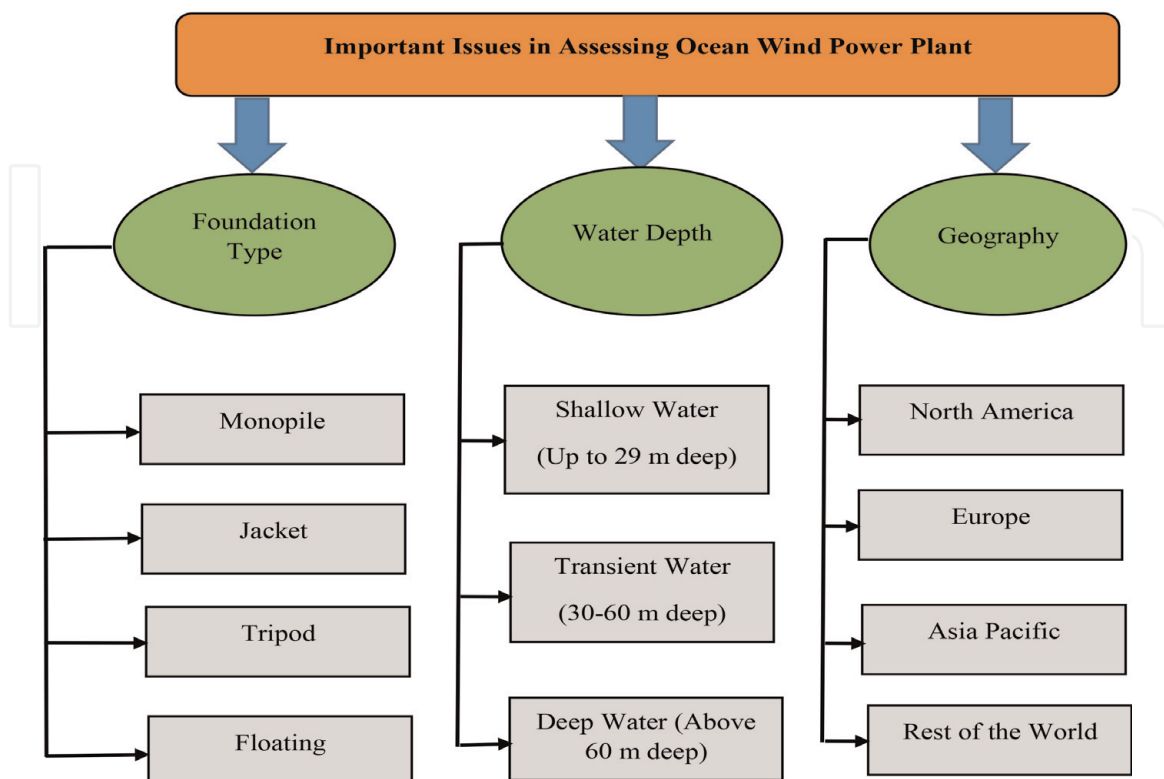


Figure 1.
Essential issues in assessing ocean wind power plant.

	Country	Planned capacity	Project name
1	China	1.5 MW	Bohai Suizhong, LiaoDong Bay
2	China	20 MW	Dongshan Island
3	China	50 MW	Hebei
4	China	100 MW	Nan'ao, southeast of Guangdong
5	China	25 MW	Shanghai Dong Mai
6	China	102 MW	Shanghai Dong Mai
7	China	100 MW	Fengxian No. 1
8	China	300 MW	Fengxian No. 2
9	China	400 MW	Nanhui
10	China	200 MW	Hengsha
11	Hong Kong	200 MW	Hong Kong offshore
12	Japan	2 × 600 KW	Setana, Hokkaido
13	South Korea	500 MW	Limjado, Jeonnam Province
14	Taiwan	4 MW	Ferry

Table 1.
Several ocean wind energy projects in Asia [5–7].

China's Five-Year Plan, five gigawatts will be added to the country's electricity grid by 2020 [4]. Taiwan also has the potential to produce electricity from ocean wind energy, and according to the plan of the Ministry of Energy, by 2025, it will be the top among the active countries in Asia that use this energy [7]. Today there are only two ocean turbines operating in the country, and two projects in a total of 320 MW are due to be installed by 2020. Japan has only 61 MW of installed energy for ocean wind energy by the end of 2016, given that it has more access to the ocean. South Korea has so far only mustered a couple of ocean wind prototypes and a single demonstration project, in a total of 35 MW [7].

1.1.2 Ocean wind energy in Europe

The European continent has many potentials for electric power generation through ocean wind energy. It is revealed that this energy will play an important role to produce electricity for Europe in the future [8].

The Netherlands started to work on offshore wind farms after Denmark [9]. Also, two ocean wind farms were built up in the Netherlands with two different capacity levels of 108 MW and 120 MW in 2006. Two new ocean wind farms were built up in Sweden by 2001 and 2002. Ireland constructed its first ocean wind farm in 2004 wind turbines of 3.5 MW. Moreover, Germany's first ocean wind farm was constructed with 20,000 MW capacity. The UK used ocean wind energy by 2000 with 3.8 MW capacity. France started to use ocean wind energy in 2005, but the construction of wind power plants for economic reasons was postponed to 2009. **Table 2** shows several offshore wind energy projects in Europe [8–10].

According to the EWEA¹, The European countries target is determining 20% of its power from sustainable sources by 2030. EWEA has set an objective to achieve 40 GW and 150 GW of ocean wind energy by 2020 and 2030, respectively. Additionally, through 2030, EWEA estimates yearly establishments of ocean

¹ European Wind Energy Association.

	Country	Planned capacity	Project name
1	Denmark	4.95 MW	Vindeby
2	The Netherlands	2 MW	Lely
3	Denmark	40 MW	Middelgrunden
4	Denmark	160 MW	Horns Rev
5	The UK	60 MW	North Hoyle
6	The UK	60 MW	Scroby Sands
7	The Netherlands	108 MW	Egmond ann Zee
8	Sweden	110 MW	Lillgrund
9	Netherland	120 MW	Princess Amalia
10	The UK	90 MW	Inner Dowsing
11	Germany	2.5 MW	Breitling
12	Ireland	25.2 MW	Arklow Bank
13	Sweden	10 MW	Yttre Stengrund
14	Italy	0.08 MW	Brindisi

Table 2.
Several offshore wind energy projects in Europe [8–10].

wind energy will be equal to 13,700 MW. Ocean wind energy will support 13.9% of total EU demand [10].

1.1.3 Ocean wind energy in Africa

Africa’s wind energy resources are focused along the coastal area and mainland shelves. These regions ordinarily have high onshore and offshore wind energy possibilities. In 2004, the African Development Bank investigated to create a wind atlas of Africa and create a quantitative guide of wind speeds over the African continents [11]. Outcomes from the investigation showed that Africa’s best wind energy is found in countries adjusted along the western, northern, eastern, and southern shores of the African continent. The special cases are landlocked countries such as Chad and Ethiopia where the topographical highlights of the land are responsible for the high wind speeds in some high-elevation zones. Additionally, according to research conducted in 2007, eight countries (Egypt, Somalia, Mauritania, Sudan, Libya, Chad, Kenya, and Madagascar) have high potential for onshore wind energy and five countries (Mozambique, Tanzania, Angola, South Africa, and Namibia) have high potential for ocean wind energy [11].

1.1.4 Ocean wind energy in America

The United States has vast ocean-wide areas such the Great Lakes, Hawaii, Alaska, and Gulf Coast with potential to use offshore wind energy to produce electricity [12]. As a result, the US Department of Energy’s, Wind Energy Technologies Office has conducted many studies on various technologies to facilitate electricity generation from wind.

According to the US Department of Energy, the USA will have 3 GW, 22 GW, and 86 GW of ocean wind by 2020, 2030, and 2050, respectively. Therefore, the USA will utilize 5.5% of its accessible ocean wind resources. The US Bureau of Energy anticipated ocean wind improvement along both the Gulf of Mexico and

	Country	Planned capacity	Project name
1	The USA	30 MW	Block Island (RI)
2	The USA	468 MW	Cape Wind (MA)
3	The USA	500 MW	US Wind (MD)
4	The USA	1000 MW	DONG Energy (MA)
5	The USA	1000 MW	Deepwater ONE (RI/MA)
6	The USA	2000 MW	Dominion Virginia Power (VA)
7	The USA	450 MW	Blue Water's Mid-Atlantic Wind Park
8	The USA	400 MW	Offshore MW (MA)

Table 3.
Several ocean wind energy projects in the USA [12, 13].

West and East Coasts, in the Great Lakes, by 2050. **Table 3** shows several ocean wind energy projects in the USA [12, 13].

1.2 Ocean wind energy technologies

In the last few decades, the technology used to exploit ocean wind energy for generating electricity has been increased day by day. These technologies depend on the geographic region, the depth of water, and the wind speed. The main parts of the ocean wind power plant include [14]:

1. Tower
2. Blades
3. Gearbox
4. Power electronic components
5. Transmission system (cables)
6. Generator

1.2.1 Ocean wind turbine blade technology

The blades of the ocean wind turbine are one of the unique parts of the wind turbine structure. They have unique mechanical and aerodynamic characteristics. Moreover, the technology of manufacturing wind turbine blades has undergone new developments in both process fields and materials used in them. As a result, manufacturers of these blades are trying to optimize mechanical properties in the aerodynamic blades by design optimization and using new materials. Composite fibers and various resins, including various materials, have been used in the production of wind turbine blade rotor.

Extraction of kinetic energy from the wind is carried out by wind turbine blades. Therefore, having an optimal design to get the most energy out of the wind is very important. Wind turbine blade design consists of two main parts. In the first step, the aerodynamic design is performed to achieve the required power rating according to the turbine wind turbine and to obtain the highest electric power

factor. In the second step, changes should be made to the blades so that the amount of aerodynamic noise generated by the blades is within the permissible range.

1.2.2 Ocean wind turbine tower technology

Wind turbine tower is the most significant, heaviest, and most expensive part of the wind turbine. Regarding the safety level, its failure can cause the entire wind turbine to fail. Proper design of the wind turbine tower significantly reduces the cost and increases the life of the wind turbine.

The tower is a cone-shaped steel structure with four segments mounted on each other by screws and flanges. The tower design includes the following main steps [15]:

- Connector analysis
- Shell strength analysis (static analysis, bending, and aging)
- Vibration analysis
- Design and selection of all internal components of the tower (entrance door, ladder, elevator, and internal platforms)

1.2.3 Ocean wind turbine gearbox technology

The purpose of using a gearbox is to transmit relatively large forces, change the torque or change the direction of rotation, or change the angle of the rotation axis. Gearboxes are increasing the nominal speed of a rotor from a small amount (a few tens of rpm) to a high value (at a rate of several hundred or several thousand rpm), which is suitable for triggering a standard generator. Ideally, the resultant value is constant in the torque at the inlet and outlet of the gearbox, but due to the energy losses in a mechanical device, torque is reduced in the output axis. In a wind turbine, the power transfer from the main rotor to the generator is usually done in three ways [16].

1.2.3.1 Direct drive transfer gearbox

In this method, the transmission is not used from the gearbox, and the torque is directly inputted from the main rotor to the generator. So, instead of using the gearbox and extending the main rotor, a generator with more poles is used. To accommodate more poles on the generator, the diameter should be increased. One of the benefits of using this design is to reduce the cost of the gearbox maintenance as well as reduce gearbox shocks and increase efficiency.

1.2.3.2 Power transfer by conventional gearbox (parallel shaft)

In this method, the power output is transmitted by a conventional gearbox to the generator. The gears used in this gearbox can be simple or spiral. To increase the upper period, it may be possible to use two or more rounds. In parallel shaft gearbox, the bearings are used to keep the gear shaft on the main body. In this type of gearbox, a helical gear is used, so in addition to radial force, the bearings must also bear a large axial force.

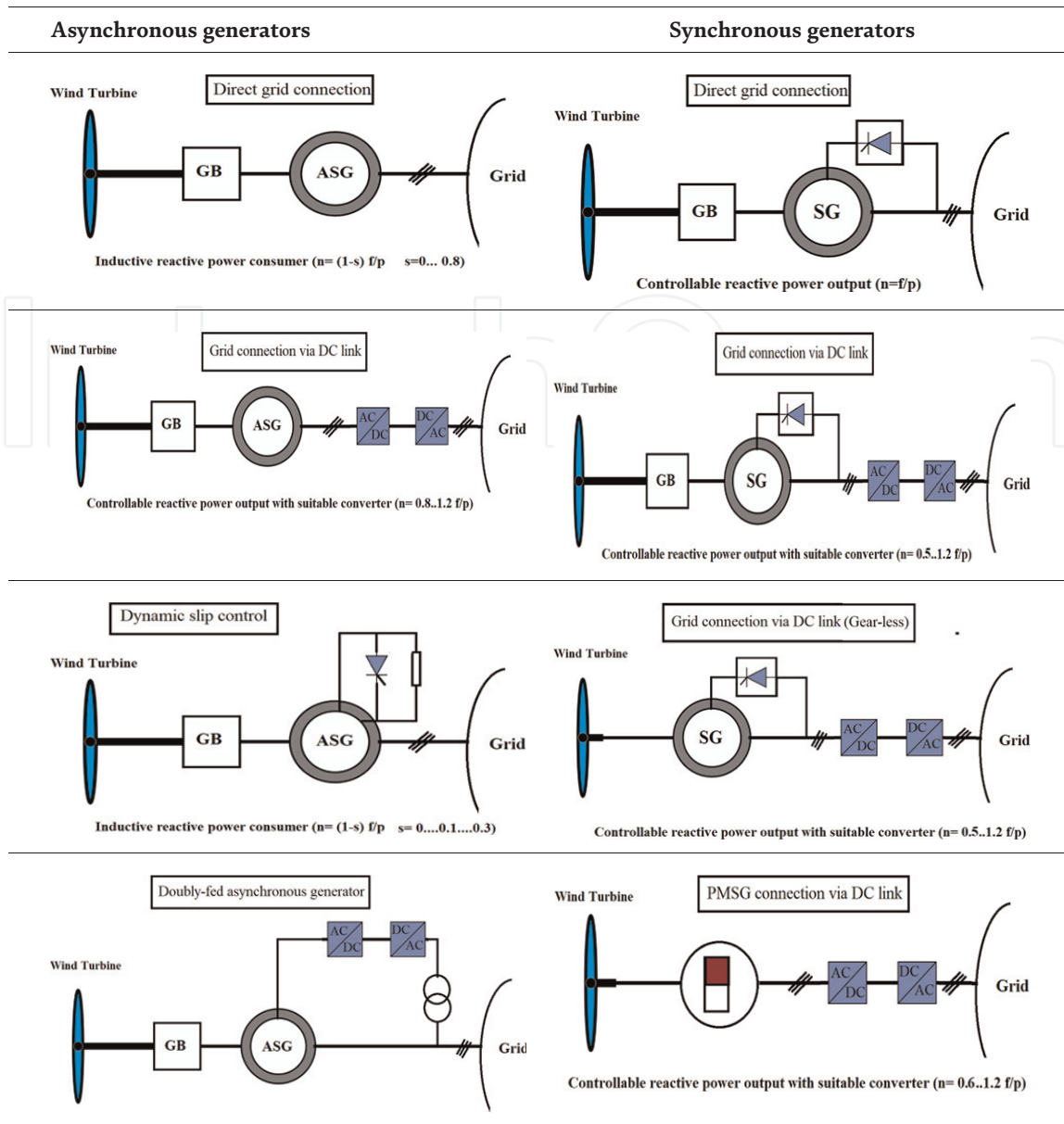


Table 4.
 Different topologies of wind energy conversion systems.

1.2.3.3 Transmission by planetary gearbox

Using this type of gearbox is very common in wind turbines. The gearbox uses three types of gears, the Sun gear in the middle, the Planetary gear, and the Ring gear, which is an internal gear. The division of force into planetary planes, reduced gearbox size, reduced slip between the gear and the planet, and increased efficiency relative to other gearboxes are benefits of the planetary gearbox.

1.2.4 Ocean wind turbine energy conversion systems

Wind turbine blades convert wind energy into rotational energy in the transmission system, and in the next step, the generator transfers the turbine's energy to the grid. The most types of electric generator part in wind turbines are asynchronous and synchronous generators. Also, DC generators have been used for some smaller turbines. **Table 4** shows the different structure of ocean wind energy conversion [17].

In general, generators used to convert energy from offshore wind farms can be divided into two main categories, which can be described as follows:

- Synchronous generator
- Induction generator
 - A. Squirrel cage induction generator
 - B. Wound rotor induction generator

1.2.5 Ocean wind turbine power transmission technology

The construction of wind farms requires a large space. Therefore, the best option for removing this limitation is the construction of these power plants in the ocean. Because the distance between offshore wind farms and the distribution network is high, it is better to use high-voltage direct current (HVDC) to transmit energy produced. The suitable transmission for ocean wind farms based on HVDC is line-commutated HVDC and voltage source converter (VSC-HVDC) [18–20]. If the length of the transmission lines is less than 50 kilometers, the use of high voltage alternating current transmission systems is not recommended. In the HVDC

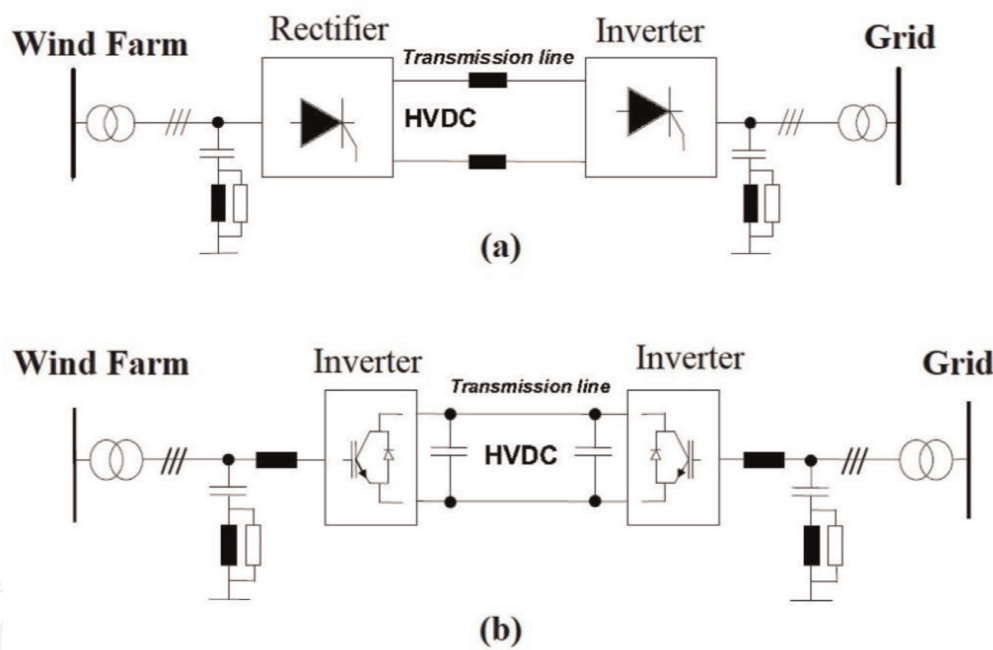


Figure 2. (a) Structure of thyristor-HVDC and (b) structure of IGBT-HVDC.

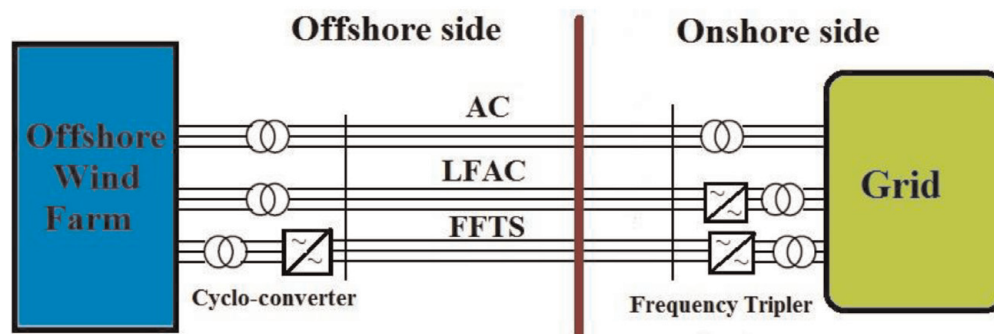


Figure 3. Different types of AC transmission line of ocean wind farm.

technology to control active power, reactive power, and voltage thyristors is replacing with IGBT (**Figure 2a** and **b**).

The HVAC transmission network is divided into different types, each with its advantages and disadvantages. The low-frequency AC transmission (LFACT) and fractional frequency transmission system (FFTS) are new transmission systems which have been used for the wind farm as a solution to cover the disadvantages of conventional AC transmission line. **Figure 3** shows a different type of AC transmission line of the ocean wind farm.

2. Active and reactive power control in the ocean wind energy system

Recently, one of the most eco-friendly and accessible renewable energy sources (RESs) being utilized all across the world is wind energy [21]. Considering the beneficial characteristic of clean energy resources such as flexible control and regulation, RESs' expansion programs and sustainable growth to reduce the greenhouse gas emissions are the main purposes of European Commission in Energy Road map 2050 [22]. Regarding the necessity of employing renewable energies, and also the remarkable global growth in the use of such energy sources, wind energy has important advantages such as zero-emission energy production and low operating costs. In spite of these benefits, there is a severe uncertainty in predicting wind speed as a big challenge for such system's integration [23]. Various machines are used in wind turbines including permanent magnet synchronous generator (PMSG), squirrel cage induction generator (SCIG), and doubly fed induction generator (DFIG). Hence, the DFIG is one of the most significant types of generators being installed in wind turbines. In DFIG, both stator and rotor are connected to the main power grid directly and by power electronic converters, respectively [24–28]. As it can be seen in **Figure 1**, the typical circuit of a doubly fed induction generator DFIG is specified, by taking into consideration the several important parts including maximum power point tracking (MPPT), rotor and grid side controllers and power electronic converters, and pulse wide modulation PWM. Both windings of the stator and rotor of the induction machine are connected to the grid directly and by power converters, respectively. To active and reactive power control, several different types of controller have been evaluated in pervious, research works. For instance, Ref. [29] uses sliding mode (SM) and PI controller, for controlling the stability and also to track reference power and remove fluctuations or active and reactive powers' disturbances. After pointing out the performance of the PI controller in the output, the obtained results are compared with a SM controller. It has been revealed that the PI controller has a more desired performance than SM controller from the output responses of the controllers' point of view. In [30], a neural-type-1 fuzzy controller is used to produced powers of wind turbine; the derived results are compared to a PI controller, specifying that the neural-fuzzy controller operates better than the PI controller. Refs. [31, 32] have used fuzzy-PI and sliding mode and also robust fuzzy-sliding mode controller (F-SMC) to control and better manage the generated Ps and Qs of the wind turbine system output. Hence, comparing of controllers' performance indicates that the output responses of the fuzzy-proportional integration controller are better than sliding mode controller. All the controllers used in the literature have been used to enhance the stability and to eliminate the fluctuation and disturbances as well as improve the reference power tracking. Furthermore, each control method has modified the pervious approaches and also improved the active and reactive powers extraction of DFIG. Another type of controller employed in DFIG generator is the fuzzy-sliding mode controller. In fact, the F-SMC is a controller which finds the best numerical values for the scaling

factor of the sliding mode. Due to the presence of fuzzy controller, all gain coefficient value is more accurate. Wind turbine operation is affected by uncertainty due to the uncertainty in the wind speed forecasts; thus the abovementioned controllers are not appropriate as they are not capable of dealing with severe uncertainties. It is noteworthy that the PI controller is point to point and type-1 fuzzy controller is able to only cover a small range of uncertainty in its outputs. By considering the high uncertainty in the wind speed, it is needed to design a controller with the capability of covering severe uncertainties. According to the control methods used in the literature, and also in order to improve and enhance the power control (Ps & Qs) in wind turbines systems, a new control method based on type-2 fuzzy logic control laws is presented. In this research, all parameters and equations are linear enabling the system designer to use MAMDANI inference system. The T2FL controller is a suitable alternative for the controlling of the powers in DFIG to deal with severe uncertainty.

2.1 Mathematical model of wind energy conversion system

Indeed, the DFIG is an induction machine which its stator and rotor is interfaced to the main power grid. The connection of the stator and electrical energy transmission from its windings to the main power grid is carried out by 3-phase power transmission lines from wind turbine to the grid. On the other hand, the rotor wounds of the induction machine are fed through the AC-DC/DC-AC back to back power converters, which received the electrical energy from 3-phase power transmission lines between stator and the main power grid. In this section, a general model is presented within a dynamic framework, by considering the variation parameters of the wind turbine based on induction machine. In this regard, the mathematical and dynamic equations are expressed as currents, voltages, and flux relations in q-d-0 reference frame and also the electromagnetic and mechanical torque. **Figure 1** illustrates the wind turbine circuit loop general operation process with controllers, in particular the rotor-side one [30, 33].

2.1.1 Universal model of the wind turbine

By taking into consideration the rate of wind speed at the different times and also due to the coefficient $(\lambda_{wind} \cdot \beta)$, the mechanical power transferred from wind turbine blades to the rotor shaft can be written as follows [27, 34]:

$$P_t = \frac{\pi \rho R^2 V_{wind}^3 C_p (\lambda_{wind} \cdot \beta)}{2} \quad (1)$$

wherein ρ is air density and R , V_{wind} , and $C_p (\lambda_{wind} \cdot \beta)$ are the radius of the turbine rotor, wind speed, and the coefficient of the power capture, respectively. Hence, the power capture coefficient $C_p (\lambda_{wind} \cdot \beta)$ can be defined as follows [33, 34]:

$$C_p (\lambda_{wind} \cdot \beta) = C_1 \left[\frac{C_2}{\lambda_i} C_3 \beta - C_4 \right] e^{\frac{-C_5}{\lambda_i}} + -C_6 \lambda \quad (2)$$

where λ_{wind} and β are denoted as ratio of the tip speed and blades pitch angle, respectively. Therefore, λ_{wind} can be calculated according to the following:

$$\lambda_{wind} = \frac{\omega_{total} \cdot R}{U} = \frac{\omega_r \cdot G \cdot R}{U} \quad (3)$$

With regard to the relation (1), the input mechanical torque of the wind turbine is obtained by following:

$$T_{\text{mech}} = \frac{P_{\text{total}}}{\omega_{\text{total}}} = \frac{\pi \rho R^2 V_{\text{wind}}^3 C_p (\lambda_{\text{wind}} \cdot \beta)}{2 \omega_{\text{total}}} \quad (4)$$

2.1.2 DFIG mathematical model theory

Generally, there are three states or significant vector models, which are used to design an induction machine called as **Park**, **Clark**, and **Concordia**. Hence, 2-phase vector model reference frame of PARK is considered for designing the induction generator. On the other hand, all relationships of doubly fed induction machine are used, is under the dynamic equations in 3-phase (a, b, c) transformation frame system to (q-d-0) 2-phase reference frame. The main parameters of formulas can be described as stator and rotor voltage, current, flux in q-d-0 system, and also electromagnetic and mechanical torque [35–38].

Figures 4 and **5** represent the vector diagram of the DFIG PARK's model and 2-phase reference frame, respectively. In these figures the conversion system from (a, b, c) reference rotating frame to (q-d-0) reference frame has been shown [32].

DFIG's voltage equations of the stator and rotor in 2-phase reference system are defined as follows [34, 37]:

$$\begin{cases} U_{d \text{ Stator}} = R_{\text{Stator}} I_{d \text{ Stator}} + \frac{1}{\omega_{\text{base}}} \frac{d\psi_{d \text{ Stator}}}{dt} - \frac{\omega}{\omega_{\text{base}}} \psi_{q \text{ Stator}} \\ U_{q \text{ Stator}} = R_{\text{Stator}} I_{q \text{ Stator}} + \frac{1}{\omega_{\text{base}}} \frac{d\psi_{q \text{ Stator}}}{dt} + \frac{\omega}{\omega_{\text{base}}} \psi_{d \text{ Stator}} \end{cases} \quad (5)$$

$$\begin{cases} U_{d \text{ Rotor}} = R_{\text{Rotor}} I_{d \text{ Rotor}} + \frac{1}{\omega_{\text{base}}} \frac{d\psi_{d \text{ Rotor}}}{dt} - \frac{\omega - \omega_{\text{Rotor}}}{\omega_{\text{base}}} \psi_{q \text{ Rotor}} \\ U_{q \text{ Rotor}} = R_{\text{Rotor}} I_{q \text{ Rotor}} + \frac{1}{\omega_{\text{base}}} \frac{d\psi_{q \text{ Rotor}}}{dt} + \frac{\omega - \omega_{\text{Rotor}}}{\omega_{\text{base}}} \psi_{d \text{ Rotor}} \end{cases} \quad (6)$$

where U.R.I. ψ is characterized as the stator and rotor voltages, resistances, and currents, fluxes in d-q reference frame, and also the rotor base speed, rotor speed, and angular speed is denoted by ω_b . ω_r . ω respectively.

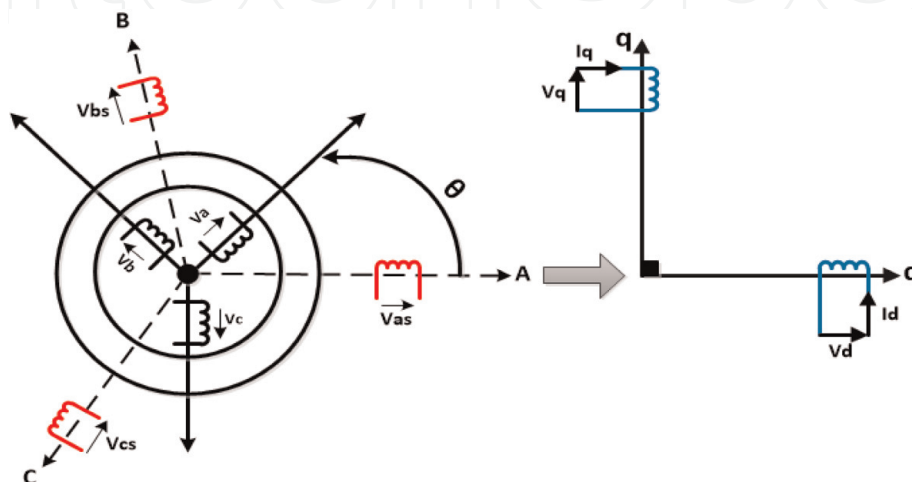


Figure 4.
 Doubly fed induction generator PARK's model [32].

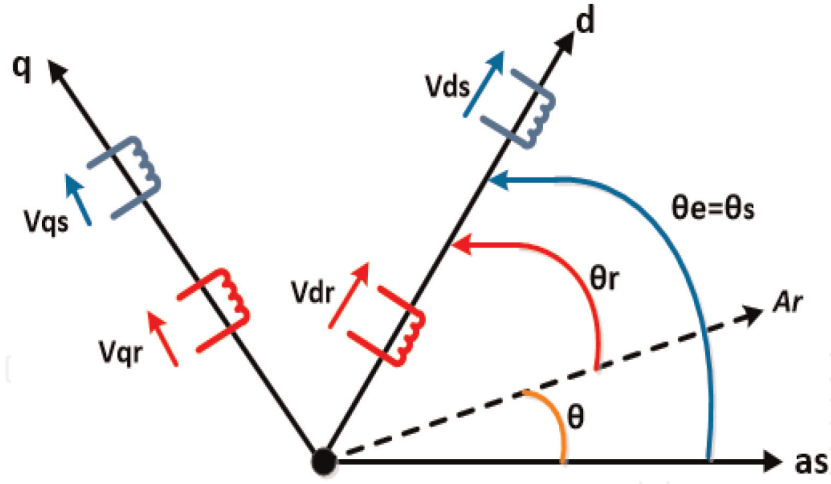


Figure 5.
The DFIG in the 2-phase reference frame [32].

Also, the induction machine's currents are in 2-phase reference frame, which are calculated as follows:

$$\begin{cases} I_{d \text{ Stator}} = \frac{\Psi_{d \text{ Stator}}}{X_{l \text{ Stator}}} - \frac{\Psi_{md}}{X_{l \text{ Stator}}} \\ I_{q \text{ Stator}} = \frac{\Psi_{q \text{ Stator}}}{X_{l \text{ Stator}}} - \frac{\Psi_{mq}}{X_{l \text{ Stator}}} \end{cases} \quad (7)$$

$$\begin{cases} I_{d \text{ Rotor}} = \frac{\Psi_{d \text{ Rotor}}}{X_{l \text{ Rotor}}} - \frac{\Psi_{md}}{X_{l \text{ Rotor}}} \\ I_{q \text{ Rotor}} = \frac{\Psi_{q \text{ Rotor}}}{X_{l \text{ Rotor}}} - \frac{\Psi_{mq}}{X_{l \text{ Rotor}}} \end{cases} \quad (8)$$

By considering current Eqs. (7) and (8), the parameters $\Psi \cdot \Psi_{Magnetic} \cdot X_{l \text{ Stator}} \cdot X_{l \text{ Rotor}}$ are known as the, flux, magnetizing flux, and stator and rotor leakage reactance in q-d two-dimensional vector space. Hence, under such condition the fluxes of the stator and rotor windings can be formulated as follows:

$$\begin{cases} \Psi_{q \text{ Stator}} = \omega_{base} \int \left(\frac{R_{Stator} (\Psi_{mq} - \Psi_{q \text{ Stator}})}{X_{l \text{ stator}}} + V_{q \text{ Stator}} \right) dt \\ \Psi_{d \text{ Stator}} = \omega_{base} \int \left(\frac{R_{Stator} (\Psi_{md} - \Psi_{d \text{ Stator}})}{X_{l \text{ Stator}}} + V_{d \text{ Stator}} \right) dt \end{cases} \quad (9)$$

$$\begin{cases} \Psi_{q \text{ Rotor}} = \omega_{base} \int \left(\frac{R_{Rotor} (\Psi_{mq} - \Psi_{q \text{ Rotor}})}{X_{l \text{ rotor}}} + \frac{\omega_{Rotor}}{\omega_{base}} \Psi_{d \text{ Rotor}} + V_{q \text{ Rotor}} \right) dt \\ \Psi_{d \text{ Rotor}} = \omega_{base} \int \left(\frac{R_{Rotor} (\Psi_{md} - \Psi_{d \text{ Rotor}})}{X_{l \text{ rotor}}} + \frac{\omega_{Rotor}}{\omega_{base}} \Psi_{q \text{ Rotor}} - V_{d \text{ Rotor}} \right) dt \end{cases} \quad (10)$$

In addition, by taking into consideration the current and flux parameters in 2-phase reference frames of the rotor and stator of the induction generator, the torques can be obtained as (11) and (12):

$$T_{electromagnetic} = \frac{1.5 P \left(\Psi_{d \text{ Stator}} I_{q \text{ Stator}} - \Psi_{q \text{ Stator}} I_{d \text{ Stator}} \right)}{2\omega_{base}} \quad (11)$$

where P , ω_{base} are the number of pole and base speed of the induction generator's rotor, respectively, which are considered in the calculation of electromagnetic torque. Due to the relation (11), the mechanical torque can be written as follows:

$$T_{Mechanical} = J \frac{d}{dt} \omega_{rm} - T_{em} + T_{damp} \quad (12)$$

In (12), the parameters T_{damp} , J are defined as the damping torque and rotor moment of inertia, considering the rotor speed variations.

2.1.3 P_s & Q_s power control process in DFIG-based WECS

The active and reactive power control strategy is that the fuzzy controller by receiving error signals and derivative of the error and also, after a control process, the signals generated through the controller is delivered to the power electronic converters and DFIG's rotor and to the active and reactive output power control of the wind turbine. The relationships of P_s & Q_s powers are defined as follows [40, 41]:

$$P_s = \left[\frac{1}{X_{l\ Magnetic}} (\psi_{d\ Stator}) + \frac{X_{Magnetic}}{X_{l\ Stator}} (1.5 I_{d\ Rotor} V_{d\ Rotor}) \right] \quad (13)$$

$$Q_s = \left[\frac{1}{X_{l\ Magnetic}} (\psi_{q\ Stator}) + \frac{X_{Magnetic}}{X_{l\ Stator}} (1.5 I_{q\ Rotor} V_{q\ Stator}) \right] \quad (14)$$

2.2 Controller design based on the type-2 fuzzy logic theory T-2FLC

2.2.1 Type-2 fuzzy controller statement

T-2 fuzzy controller is a developed controller in that its operation strategy is under the uncertainty. Therefore, this type of controller is appropriate for systems with high uncertainty such as wind or solar power plants, which the generation is exactly under the pure uncertainty. The performance of the T2FLC because of covering a large scale of high uncertainty to control the wind turbine parameters is more desired than the T1 fuzzy or another controller technique. Structurally, both T1 and T2 fuzzy controllers are the same, but with this difference in the interior structure of T2FLC, due to the presence of uncertainty, there is a section as type reducer (TR). The calculation and the conversion of the type of fuzzy from type 2 to type 1 are the important functions of the TR section. Depending upon the linearity and nonlinearity of the model, two types of inference system exist in T2FLC. The MAMDANI inference system is used for the systems with linear equations, and TSK inference system is employed for the systems with nonlinear equations.

2.2.2 Extended fuzzy sets

Generally, T2 fuzzy sets are extended of type-1 fuzzy sets. On the other hand, T2FS is a fuzzy set with membership degree of fuzzy. Type-2 fuzzy sets can compensate the limitation of type-1 fuzzy sets in covering uncertainties as a new method with its specific advantages. Forasmuch as fuzzy sets are defined based on linguistic variables, thus the T2FS is appropriate to model uncertainty process using linguistic variable. The primary membership grade in T1FSs is a crisp number in $[0, 1]$, whereas the primary membership grade in T2FSs is a T1FSs in range of

In order to reduce the computational complexity, the interval fuzzy sets (IFSs) are proposed as an alternative to the general fuzzy sets (GFSs). Hence, a set (\tilde{H}) of interval type2 is defined as follows:

$$\begin{cases} \tilde{H} = \int_{y \in Y} \int_{v \in Z_y} \frac{1}{(y.v)} Z_y \subseteq [0.1] \\ \tilde{H} : Y \rightarrow \{[E.F] : 0 \leq E \leq F \leq 1\} \end{cases} \quad (16)$$

The performance of fuzzy inference engine is under the considered rules. With seven membership functions, 49 of the commands written to form IF-THEN have been considered as represented in **Table 1** [37–42]. The relation of footprint of uncertainty is as follows:

$$\text{FootPrintin}(\tilde{H}) = \cup_{y \in Y} Z_y = \{[y.v] : v \in Z_y \subseteq [0.1]\} \quad (17)$$

According to the impacts of the uncertainty in FT2 sets, the bound of FT2 sets includes two fuzzy type-1 set membership functions as upper membership function (UMF) and lower membership function LMF. The embedded fuzzy sets in the set of H can be defined as follows as a \tilde{H}_e set [18]:

$$\tilde{H}_e = \int_{y \in Y} \frac{[1]}{y} . v \in Z_y \quad (18)$$

2.2.3 Principle process of the type-2 fuzzy logic inference system

The general performance of T2FLC is based on rules and relationships which have been considered for it. As it can be seen in **Figure 8**, the principle process of type-2 and type-1 fuzzy control systems are the same, but with this difference that the FT2 control system has a unit called fuzzy type reducer. FT2 system comprises five important parts in that the first part is the fuzzifier unit, while the inputs of [0, 1] interval are converted to fuzzy sets. The second part is the inference engine unit wherein; all fuzzy sets are inferred by rule base unit, simultaneously. Depending upon linearity or nonlinearity of the fuzzy control inputs and the equations, the inference system in (T2FLS) control system can be MAMDANI or TSK. The next part after the inference engine taken into consideration the most important part of FT2 logic system is the rule base unit. All fuzzy inference calculations are according to the human knowledge and written in the frame of IF-THEN.

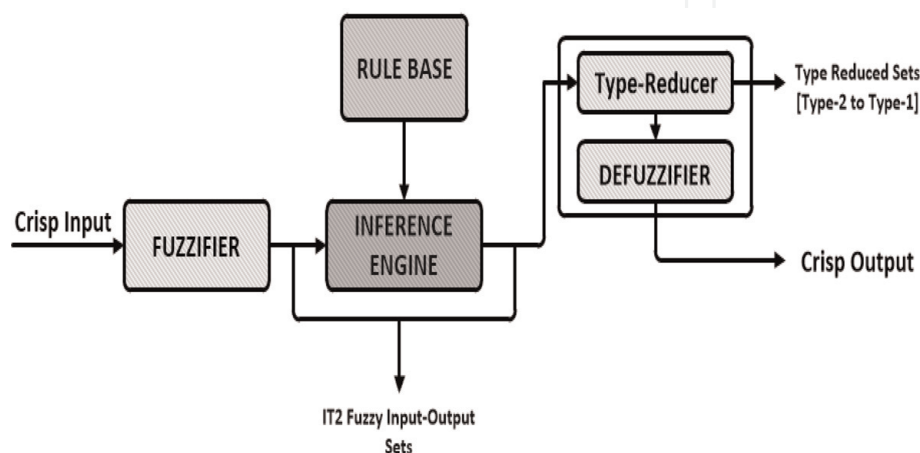


Figure 8.
 Overall process of FT2 logic system.

The fourth section of FT2 system is the type reducer. Since the FT2 sets are based on the uncertainty and due to the high computational burden of the fuzzy system, this is not possible for the system output to be converted to $[0, 1]$ directly. First, all the sets of the FT2 are converted to FT1 sets using the type reducer and then applied to the defuzzifier unit and converted to $[0, 1]$ in the output. The last part of the FT2 system is the defuzzifier unit in that its performance is in the opposite way of the fuzzifier system and converts all fuzzy sets to $[0, 1]$ [38–40].

By taking into consideration the significant parts of type-2 fuzzy topology, the process of inference is expressed in the form of mathematical, which is denoted as follows:

$$E^M = [F_{Lower} \cdot F_{Upper}] \quad (19)$$

subject to

$$F_{Lower}^M = \min \left[\left(\mu_{N_1^k} \right)_{Lower} (y_1) \dots \left(\mu_{N_p^k} \right)_{Lower} (y_p) \right] \quad (20)$$

$$F_{Upper}^M = \min \left[\left(\mu_{N_1^k} \right)_{Upper} (y_1) \dots \left(\mu_{N_p^k} \right)_{Upper} (y_p) \right] \quad (21)$$

And the minimum and maximum computational of type reducer can be expressed in the fractional functions as follows:

$$Z_l = \min_{\delta_i \in [F_{Lower}^K(x_i) \cdot F_{Upper}^K(x_i)]} \frac{\sum_{i=1}^N x_i \delta_i}{\sum_{i=1}^N \delta_i} \quad (22)$$

$$Z_r = \max_{\delta_i \in [F_{Lower}^K(x_i) \cdot F_{Upper}^K(x_i)]} \frac{\sum_{i=1}^N x_i \delta_i}{\sum_{i=1}^N \delta_i} \quad (23)$$

Finally, defuzzification is the next step after the type reduction unit which in order to achieve the controller's output is done by:

$$Z_c = \frac{Z_l}{2} + \frac{Z_r}{2} \quad (24)$$

2.2.4 Type-2 fuzzy controller design

Generally, **Figure 9** shows the process of the data inference, analyze and conversion them from crisp system input $[0, 1]$ to the type-2 fuzzy system and again transform to the crisp system output $[0, 1]$. According to the main system's input equations, the design of FT2 controller has been done using the FT2 toolbox. The FT2 controller detail, such as error, change of error that is gain input (KP, KD), fuzzy inference system unit, output gain (KU) with its intervals, the number of considered membership functions for inputs and output, some of its laws, and, also, the type of inference, is expressed in the form of a toolbox. Given the linearity of the equations of DFIG, the MAMDANI inference system with Gaussian membership functions has been considered for the FT2 controller [39]. The main part of type-2 controller is the fuzzy inference (FIS) section, in which all operating levels of fuzzy sets can be done by this part. Since this work is focused on the rotor-side controller RSC and also by considering the presence of uncertainty in the wind speed, elimination of the oscillation (overshot), as well as stability enhancement of the output powers P_s & Q_s of the wind turbine based on DFIG, is the principal target of this essay. With regard to **Figure 1** that indicated the general structure of

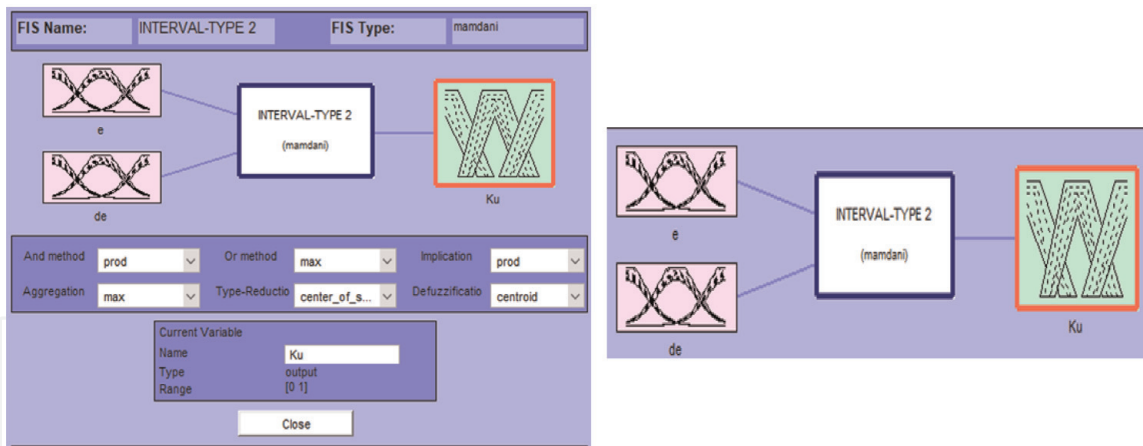


Figure 9.
 Type-2 fuzzy logic toolbox.

the DFIG, hence, as it can be seen, the type-2 fuzzy controller input parameters are the active and reactive powers, and its output is the voltage of the rotor in the q-d-0 reference frame. The performance of fuzzy inference engine is under the considered rules. With seven membership functions, 49 of the commands written to form IF-THEN have been considered as represented in **Table 1** [37, 38, 40]. To better indicate the concept of the type-2 toolbox and its application to T2FL controller design, the general scheme of an interval type-2 toolbox with MAMDANI inference strategy and also the type of inputs and output membership functions with its ranges are depicted in **Figures 5** and **7**, respectively. As shown in **Figure 8**, the structure of type-2 fuzzy logic controller is composed of input gains (KP, KD), type-2 fuzzy inference unit, output gain (KU), and plant as well. Indeed, the plant section is a mathematical transfer function. Since the type-2 fuzzy inference section is the main part of T2 controller and on the other hand its function is directly based on the IT2 toolbox, thus, under such conditions, it is required that all parameters' information about the type-2 controller system, such as input and output scaling factors, number of rules and command, membership functions, and its ranges, are defined in the toolbox as well. All sections of the T2 fuzzy logic controller are shown in **Figure 10**.

Notation 1: Each letter in **Table 5** has a special meaning. For instance, negative big (NB), negative medium (NM), negative small (NS), zero (ZO), positive small (PS), positive medium (PM), and positive big (PB).

As shown in **Figure 11**, the structure of type-2 fuzzy logic controller is composed of input gains (KP, KD), type-2 fuzzy inference unit, output gain (KU), and plant as

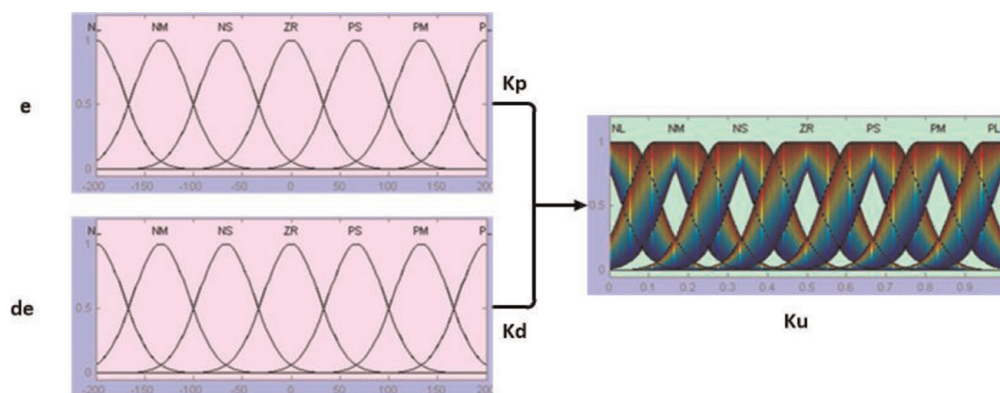


Figure 10.
 Input and output Gaussian membership functions with its intervals.

E/COE	NB	NM	NS	ZO	PS	PM	PB
NB	NB	NB	NB	NM	ZERO	ZERO	ZERO
NM	NB	NB	NB	NM	ZERO	ZERO	ZERO
NS	NB	NB	NB	NM	ZERO	ZERO	ZERO
ZO	NM	NM	NM	ZERO	PM	PM	PM
PS	ZERO	ZERO	ZERO	PB	PB	PB	PB
PM	NB	NM	NS	PM	PB	PB	PB
PB	PS	PM	PB	PB	PM	PB	PB

Table 5.
Type-2 fuzzy rule chart.

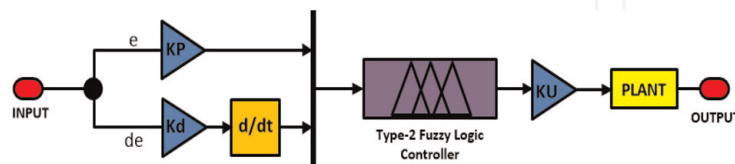


Figure 11.
The main structure of the type-2 fuzzy logic controller simulation.

well. Indeed, the plant section is a mathematical transfer function. Since the type-2 fuzzy inference section is the main part of T2 controller and on the other hand its function is directly based on the IT2 toolbox, thus, under such conditions, it is required that all parameters' information about the type-2 controller system, such as input and output scaling factors, number of rules and command, membership functions, and its ranges, are defined in the toolbox as well. All sections of the T2 fuzzy logic controller are shown in **Figure 11**.

Each of letters in **Table 1** has a special meaning. For example, negative big is the meaning of NB, and ZO is the abbreviation of zero, while the following describes the fuzzy rules:

If error is **negative big** and change of error is **negative big**, then KU is **negative big**.

2.2.5 Tuning of FT2 controller's gains using the PSO algorithm

PSO is one of the most popular optimization algorithms which is operated according to the social treatment of birds and aquatics movement. The process of optimization in the algorithm ends whenever using the pre-defined stop criteria [43, 44]. In this article, (PSO) algorithm is used to tuning the input and output scaling factors of the controller. To optimize the output powers (Ps & Qs) of the wind turbine through the T2 fuzzy controller, it is required to properly tune the input and output gains of the controller [45–47]. Under such conditions, each of the input and output scaling factors of the type-2 controller will have a suitable number, in which its numerical amounts are determined by PSO algorithm. In the presence of uncertainty and due to the complexity and the large number of the FT2 equations, it would be very difficult or even impossible to choose an optimal number or enter values manually into the input and output gains. Accordingly, PSO algorithm has been used in this paper to accelerate adjusting the coefficients to get the proper number and more accurate response to regulate the input and output scaling factors of the controller. The PSO algorithm is based on the particles' behavior including the velocity and the location of particles [48–53]. Taking into consideration the general structure of the PSO algorithm, the process of coefficients regulation of the

FT2 controller's input and output gains using PSO algorithm is defined in three steps. At the first step, a general cost function is created including the names of the controller's gains characteristic; the name of the main system that the type-2 fuzzy controller is considered for, i.e., a DFIG-based wind turbine; and the sum of error and the change of the error. In the second step, the main values such as the number of parameters, the minimum and maximum values of the input and output of the FT2 controller gains (KP, KD, KU), the name of the cost function, the number of maximum iteration, as well as all parameters relating to the PSO algorithm are defined. In the third step, the best numerical value of the FT2 controller gains is determined by running the PSO algorithm. By considering a larger number of iteration loops in the algorithm to adjust the gains of the controller, the output response will be improved. The general structure process of the type-2 controller's gain regulation has been depicted in **Figure 12**. As shown in **Figure 9** and also with the presence of the T2 fuzzy controller in this system, the PSO algorithm adjusts all scaling factors of the T2FL controller by receiving the error and change of error (E, COE) as the input and then chooses the best value for each gain of the controller (KP, KD, KU) in the output. To better understand the optimization procedure by the PSO algorithm, all the algorithms' steps are described as a flowchart in **Figure 13**.

Notation 2: Indeed, the PSO algorithm is based on the cost function for which it is intended. In order to membership functions tuning of the type-2 fuzzy controller gains, the cost function is defined as follows:

```

Function H= Cost Function-FCN (KP, KD, KU)
Sim ('DFIG')
H=Sum ((e. ^ 2) + (De. ^ 2))
End
    
```

2.3 Simulation results

This part expresses the simulation results obtained using the presented framework. In this regard, the obtained results using the proposed FT2 controller are compared with those obtained by the FT1 controller. **Figure 14(a)** and **(b)** shows the error and change of error surfaces of the FT1 and FT2 controllers, respectively. In this regard, the FT2 controller has a smoother surface than FT1 due to the covering uncertainty in a large and different ranges and high computational burden. This paper is focused on the power (P & Q) control using the RSC. According to the circuit loop of doubly fed induction machine, the general power control process in

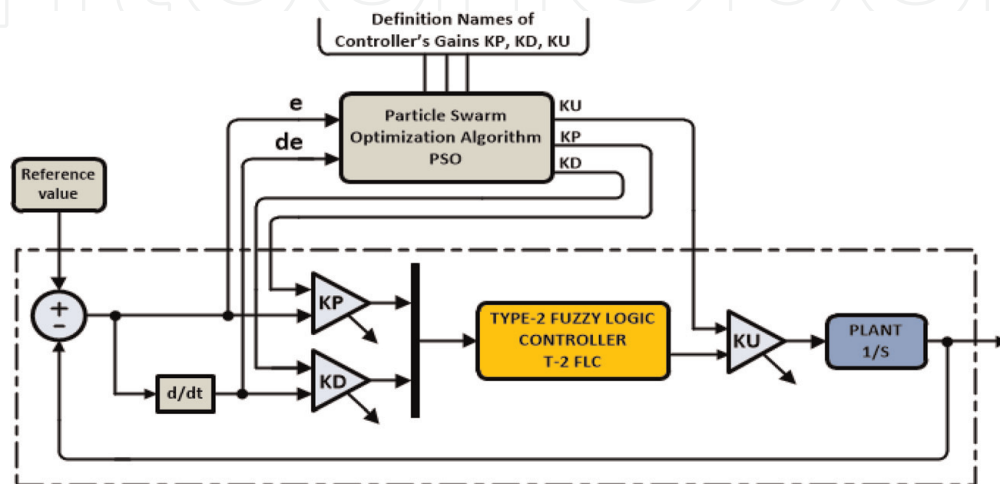


Figure 12.
 Tuning of fuzzy type-2 controller gain process using PSO algorithm.

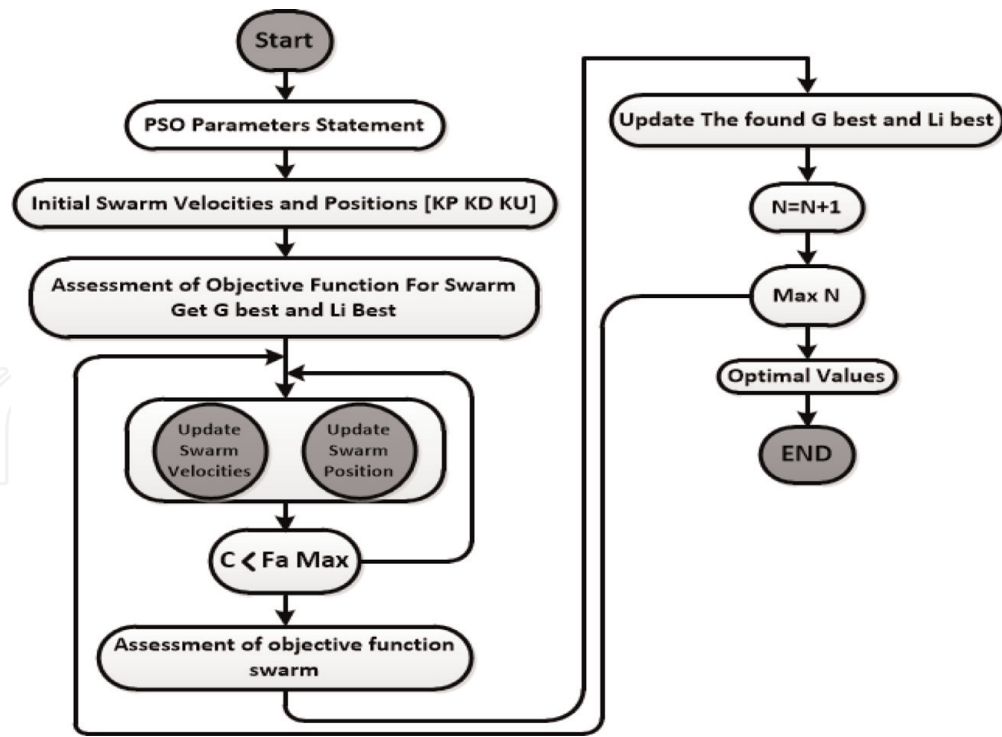
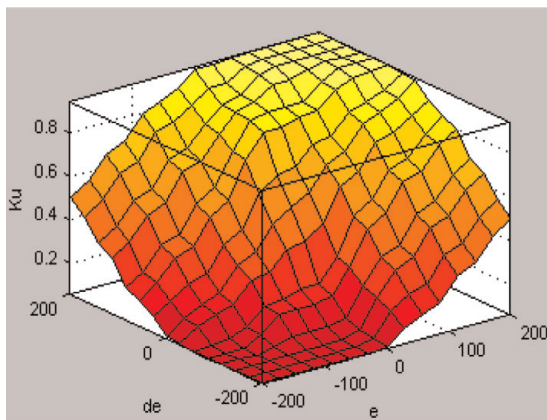
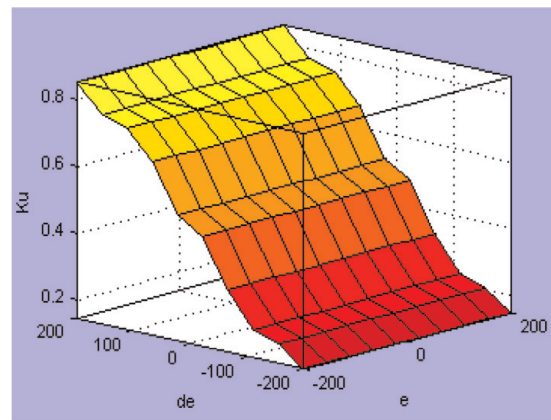


Figure 13. Flowchart of the PSO algorithm.



(a)



(b)

Figure 14. (a) and (b), The FT1 and FT2 control surface.

the DFIG-based wind turbine can be stated in multiple stages. At the first stage, after entering the value of the measured power (the generated power by the DFIG in the initial moment without controller's function), reference power is compared by the type-2 fuzzy controller. Regarding the transfer function considered for the T2 FLC, the output signal of the controller is the rotor voltage in $d-q$ reference frame. Since the input of pulse wide modulation (PWM) unit is the voltage in the a, b, c reference frame, at the second stage, first the controller's output voltage in $d-q$ frame is converted to the a, b, c frame by a $d-q$ to a, b, c unit transformation; after that the controller's output signal will be sent to the PWM block, and at the third stage, the output signal of the PWM will be transferred to the rotor-side power converter. In the presence of uncertainty of the wind speed, the main goal of this simulation is to show the stability of the powers on the considered reference numerical amount, using a T2 fuzzy controller. In order to power stability on the value of 400 W, the reference power should be adjusted to 400. The active and reactive power output responses have been exactly stabilized at the reference

amount which is considered for the outputs of the T1 and T2 fuzzy controllers. All the results are depicted in **Figures 15** and **16**. As it can be seen in the figures, both the powers P_s & Q_s are in the stable mode after multiple overshoot in the transient state of the FT1 controller output, but in FT2 controller, the active and reactive powers have been stabilized without any overshoot or oscillation in the transient state. Indeed, before the active power and reactive power are stabilized in the output, all overshoots or disturbances are removed in the transient states by the FT2 controller. In the FT2 controller due to the high computational burden, the active and reactive powers become stabilized with more latency compared to the FT1 controller. In this part, to better indicate the wind turbine and also for more

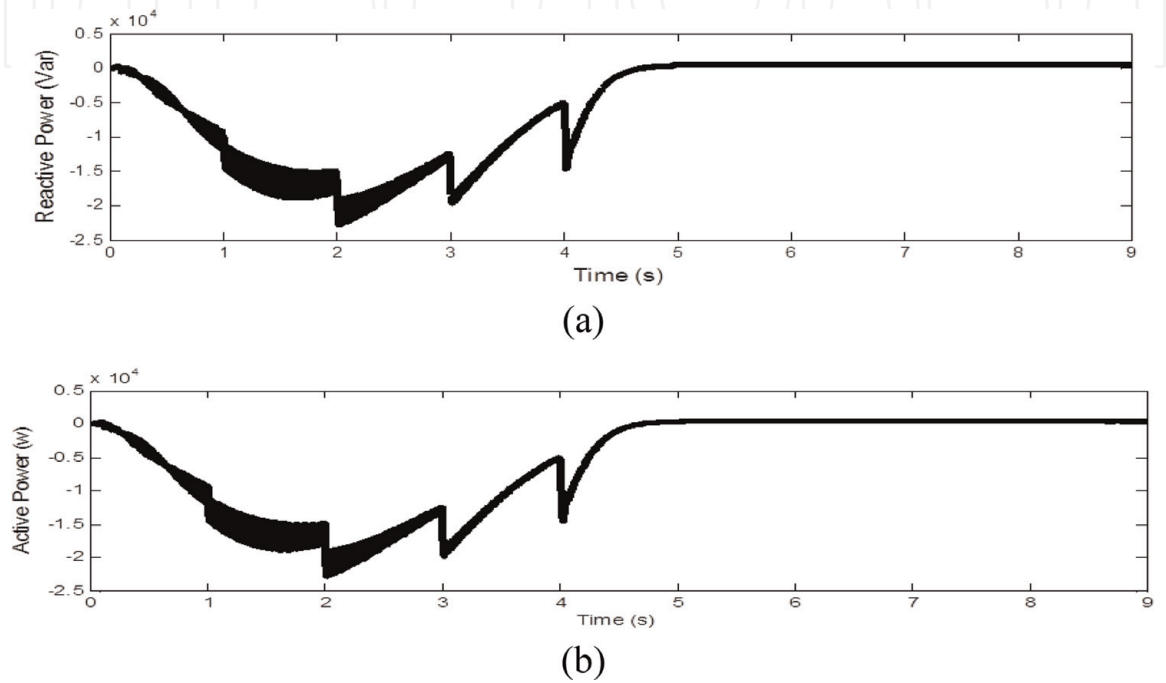


Figure 15. (a) and (b). The output results of the active power (a) and reactive power (b), controlled using the FT1 controller.

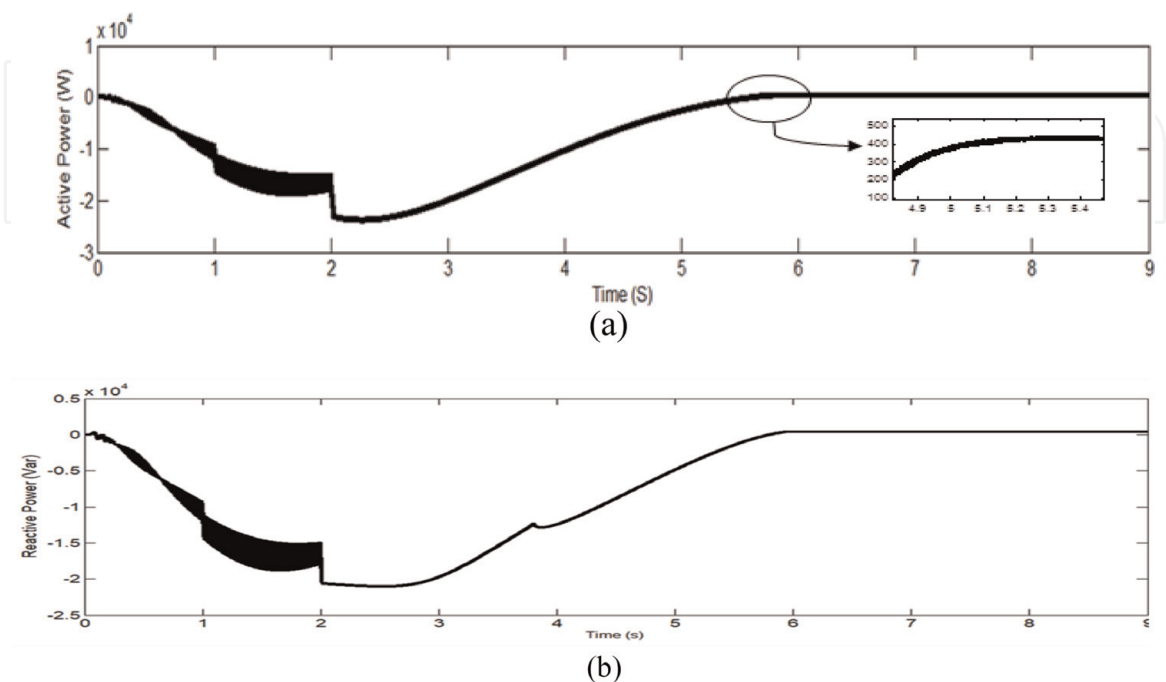


Figure 16. (a) and (b). The active power (a) and reactive power (b) output control using the FT2 controller.

Parameters	Acronyms	Numerical values
Frequency	(F)	60
Stator line voltage	($V_{L(rms)}$)	200
Stator resistance	(R_S)	3.35
Rotor resistance	(R_r)	1.99
Stator leakage inductance	(L_{LS})	$6.94e^{-3}$
Rotor leakage inductance	(L_{Lr})	$6.94e^{-3}$
Magnetic inductance	(L_M)	$163.73e^{-3}$
Moment inertia	(J)	0.1
Number of pole	(P)	4

Table 6.

Numerical values of the main parameters of the DFIG with its acronyms.

information, all the numerical values of the main parameters of the DFIG design with its acronyms are organized in **Table 6**. The DFIG numerical amount chart consists of voltage, resistance, inductance leakage of the rotor and stator, magnetic inductance, moment inertia, and the number of poles.

Notation 3: Since, in this paper, the main control aim is sustainable of the output powers without any fluctuation or is less overshoots at the reference value; hence, the numerical value 400 W is considered for both controllers, as the reference amount.

2.3.1 P & Q powers controlled using type-1 fuzzy controller

With regard to **Figure 15(a)** and **(b)**, both powers P_s and Q_s of the type-1 controller's output, until reaching to the stable conditions, have faced multiple oscillation (overshoots) in its transient state, and also, by taking into consideration the presence of uncertainty, the powers are stabilized at the reference amount 400 W. The FT1 controller just covers a small interval in its output, and as the performance of the main system which is based on the uncertainty, the FT1 controller would not be able to properly control the output powers because of the presence of uncertainty, in which the transient states of FT1 controller output are with multiple fluctuations. However, multiple fluctuations occur in the FT1 controller's output mainly due to the uncertainty.

2.3.2 P_s & Q_s powers controlled using type-2 fuzzy controller

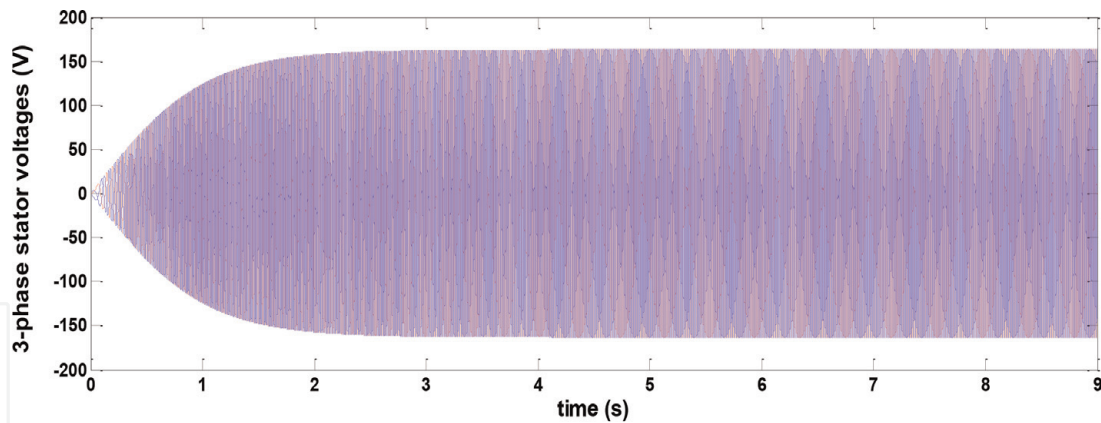
Figure 16 demonstrates the active and reactive powers outputs. Therefore, as shown, the performance of T2 controller is better than T1 controller; in other words, the powers have improved in its transient mood by considering the presence of the uncertainty, and on the one hand, T2FLC has a smoother surface in its control of the output powers. Since the computational burden of the mathematical theory of the type-2 fuzzy strategy is high, the output response of the FT2 controller until the stable state is associated with a time delay of several seconds. Due to the capability of the FT2 controller in covering a large range of the uncertainty, fluctuations have been removed, and it presents a smoother behavior in its transient state. In this paper, as previously described, with a little time delay, both P & Q power outputs of the FT1 and FT2 controller are stabilized at the value of 400 W. The stability of the active and reactive powers at the reference value has been depicted

in **Figure 16(a)** and **(b)**, respectively. P_s and Q powers output response of T1FLC indicates the controlled output power stability at the pre-defined reference value in **Figure 13**. As specified in **Figure 16(a)**, it has been shown that the active power is stabilized at the value of 400 W. By taking into consideration the type-1 and type-2 controller functions, the major difference between them is to cover the uncertainty. The T1 controller cannot cover uncertainty, or in other words, it just controls the powers over a small specified range, while the T2 fuzzy controller can cover the uncertainty in large scales.

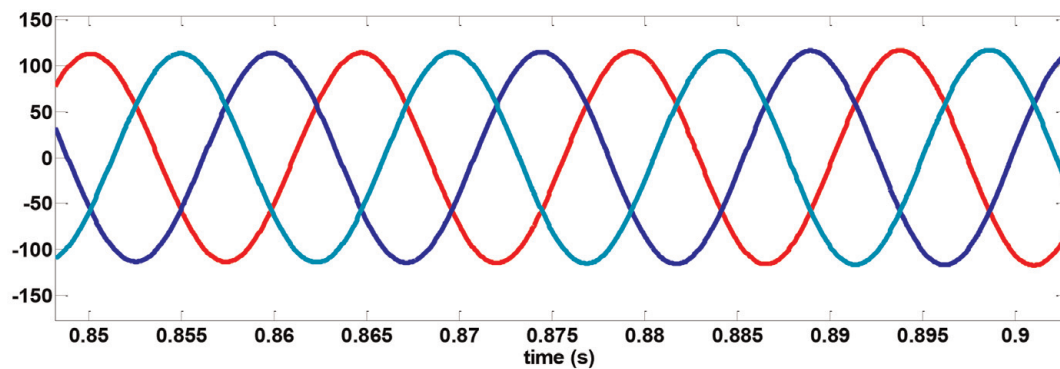
Both active power and reactive power output response of the type-1 FLC indicate the controlled output power stability at the pre-defined reference value in **Figure 16**. In **Figure 16(a)**, it has been shown that the active power is stabilized at the value of 400 W. Regarding the functions of type-1 and type-2 fuzzy controllers, the major difference between them is to cover the uncertainty. The T1 controller cannot cover uncertainty, or in other words, it just controls the powers over a small specified range, while the T2 fuzzy controller can cover the uncertainty in large scales.

2.3.3 Voltages [$U_{as} U_{bs} U_{cs}$] and currents [$I_{as} I_{bs} I_{cs}$] of the stator

In this section, the results of 3-phase voltage and currents between DFIG's stator and the main power grid through the power transmission lines have been investigated. Hence, the results of the stator 3-phase voltages are characterized in the frame of [$U_a U_b U_c$]. Also, in order to show the numerical range of sinusoidal output of the wind turbine, the numerical value 200 V is intended for the output system. **Figure 17(a)** indicates that the output voltage of the DFIG's stator is in the range of

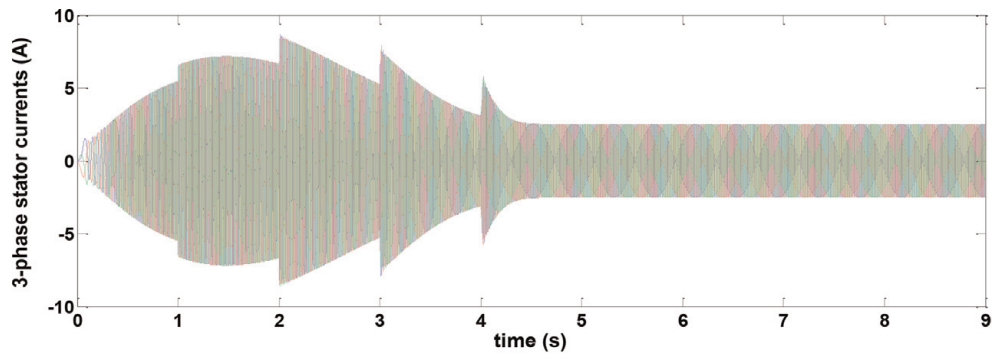


(a)

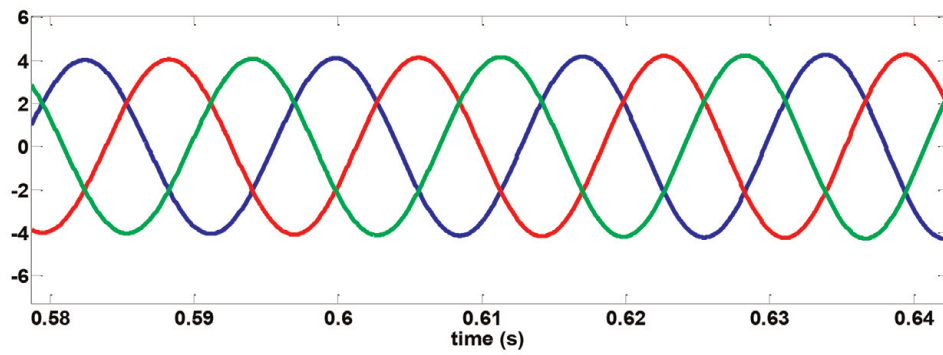


(b)

Figure 17. (a) and (b). 3-phase voltages from grid to the stator in (a, b, c) reference frame with the sinusoidal waveform.



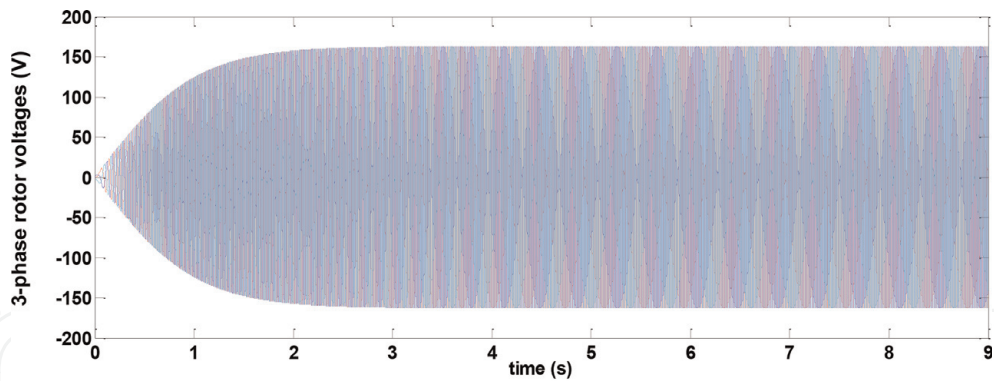
(a)



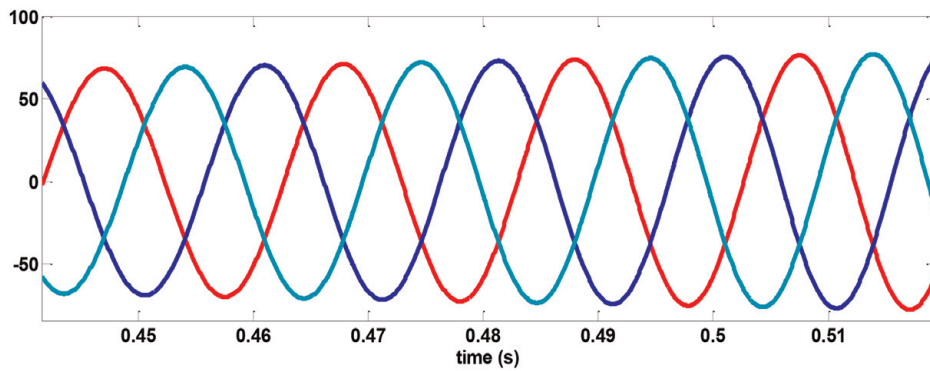
(b)

Figure 18.

(a) and (b). 3-phase currents of the stator in (a, b, c) reference frame with sinusoidal waveform.



(a)



(b)

Figure 19.

(a) and (b). 3-phase rotor voltage with sinusoidal waveform.

(−200, +200) exactly. So, the sinusoidal waveform of the three-phase voltages has specified in **Figure 14(b)** clearly. **Figure 18(a)** illustrates the stator current response by taking into consideration the range of (−10, +10). Generally, the waveforms of the stator 3-phase currents are sinusoidal as well, which have been depicted in **Figure 18(b)**.

2.3.4 Voltages [$U_{ar} U_{br} U_{cr}$] of the rotor

The input of the PWM is the voltage in [$a_r b_r c_r$] frame. Regarding the input voltages of the rotor, which will be in a, b, c frame, therefore, before the delivery of the signal from controller to the PWM, the output of the FT2 controller that is the voltage rotor in $d-q-0$ frame should be converted to a, b, c reference system. The interval of the rotor's 3-phase voltage depends upon the considered value. In this paper, the desired numerical amount is (200 V). **Figure 19(a)** represents the three-phase rotor output voltage that is stable in the range of [−200, +200]. The value of the PWM unit input voltage must be in per unit. In principle, the rotor voltage waveform is sinusoidal which has been depicted in **Figure 19(b)**.

3. The possible structure of an offshore wind turbine

In general, the structure of ocean wind farms can be divided into two main categories:

1. From the perspective of the foundation used for construction
2. From the depth of water view

This chapter addresses the above issues.

3.1 Offshore wind turbine from foundation point of view

Offshore turbines are placed in the water and have more complexity to install on a turbine mounted on the land. **Figure 20** shows the different foundations for ocean wind turbines. Additionally, offshore wind turbine foundation must withstand harsh condition as well. This explains the wide variety of foundation developed over the years for offshore turbines, some more proven than others [54].

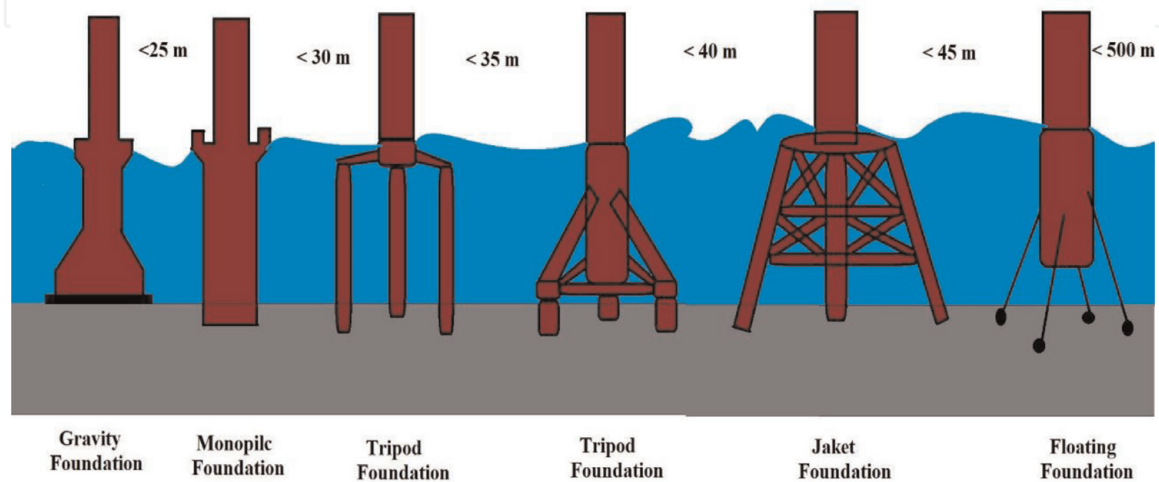


Figure 20.
 The different foundations for ocean wind turbines.

3.2 Offshore wind turbine from the depth of water point of view

The layout of offshore wind farm changes based on the geographic area, the structure of the wind turbine, and the depth of water. The structure of water turbines in shallow water, deepwater, and floating has been investigated.

3.2.1 Shallow water offshore turbine

For areas with a water depth of fewer than 40 m, the use of offshore wind farms is appropriate.

Figure 21 shows the typical structure of shallow water wind turbines:

- A. Gravity base
- B. Mono-pile
- C. Mono-caisson
- D. Multi-pile
- E. Multi-caisson

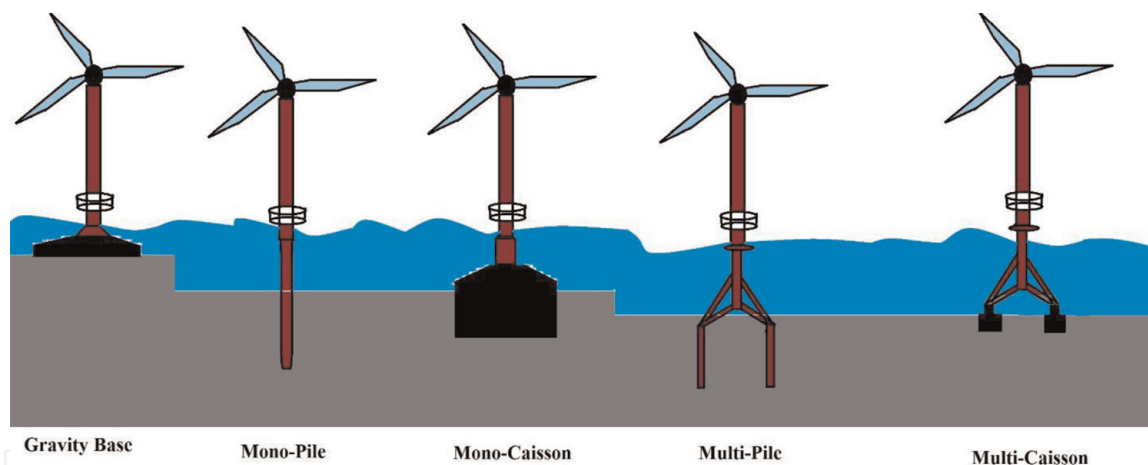


Figure 21. Models of ocean wind turbines in shallow water.

3.2.2 Deepwater offshore wind turbine

For areas with a water depth of more than 40 m, the use of low wind turbine is appropriate. **Figure 22** shows the typical structure of deepwater wind turbines:

- A. Tripod tube steel
- B. Guyed tube
- C. Spaceframe
- D. Talisman energy concept

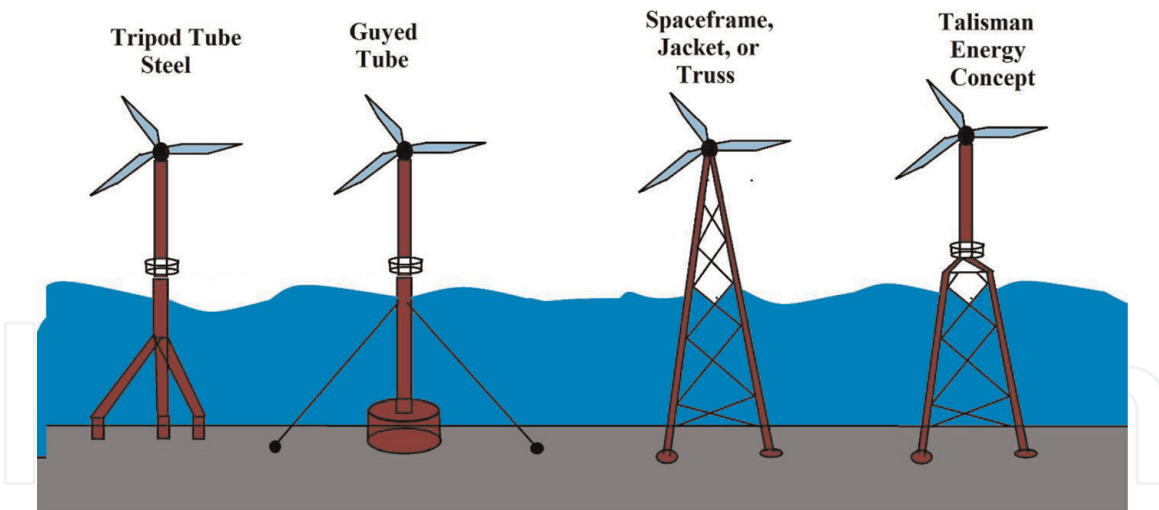


Figure 22.
Models of ocean wind turbines in deepwater.

3.2.3 Floating offshore wind turbine

Floating wind turbines are constructed on a floating structure on water, which is kept in different ways on the ocean floor. This method is used in areas where it is not possible to make a foundation for them. **Figure 23** shows three types of floating structures in an offshore wind turbine.

1. Tension leg mooring systems
2. Catenary mooring systems
3. Ballasted catenary configuration

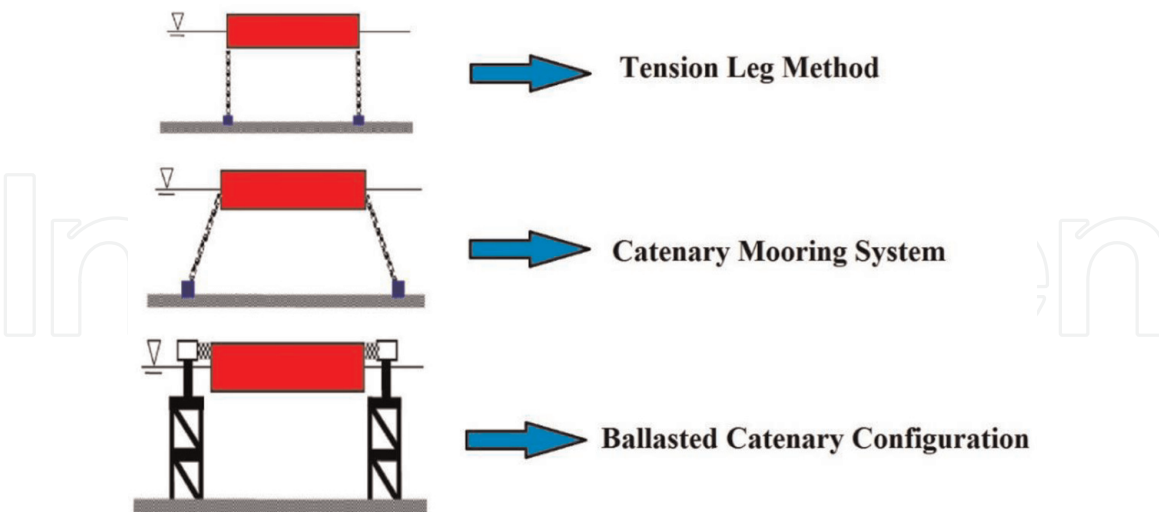


Figure 23.
Three types of engineered design for anchoring floating structures.

3.3 Offshore wind farm design

The design of offshore wind farms should be considered from three crucial points. **Figure 24** shows the design process for a typical ocean wind turbine.

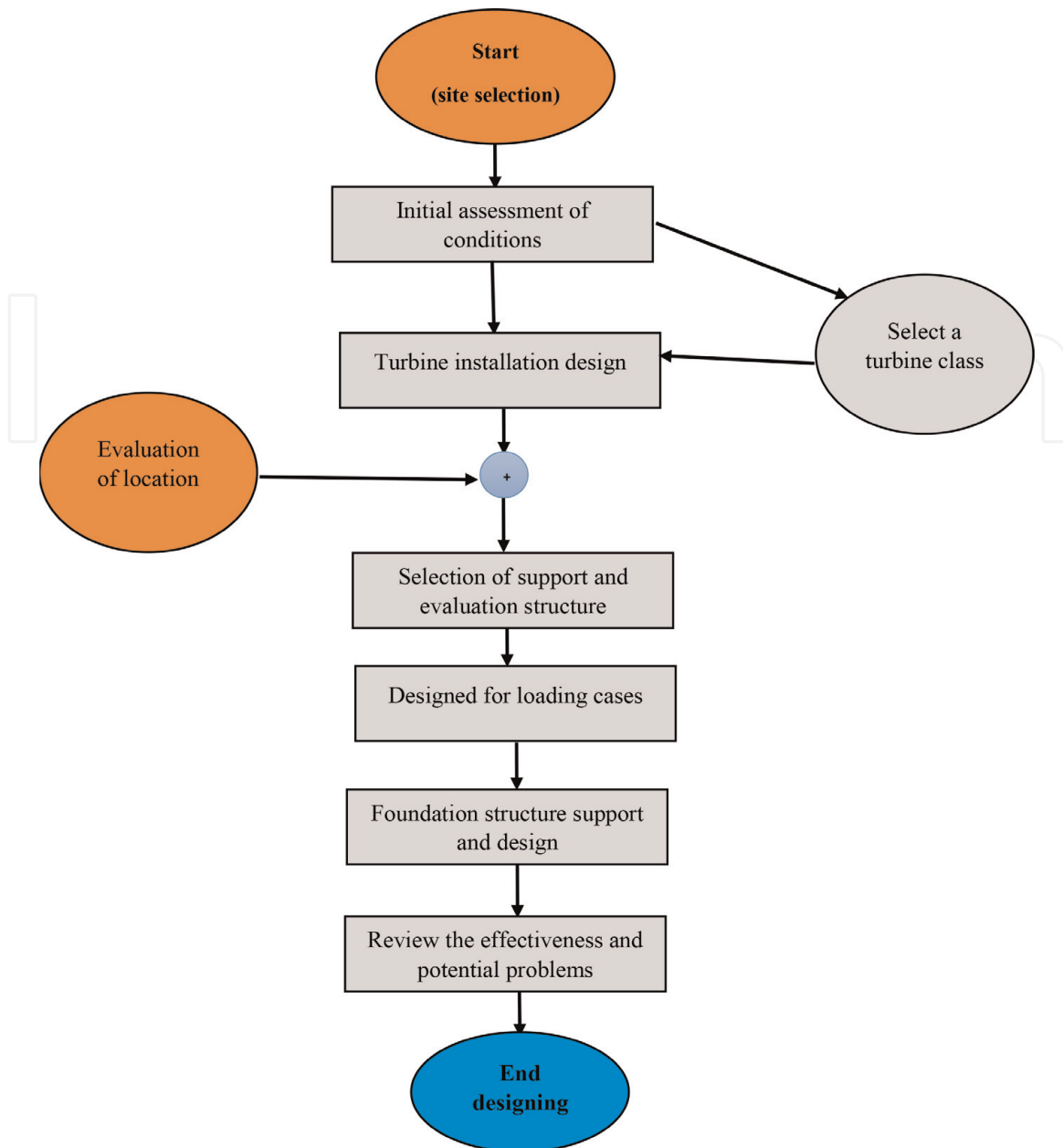


Figure 24.
The design process for a typical ocean wind turbine.

4. Challenges of offshore wind power plants

In general, two types of offshore wind power plant structures are challenging, (i) fixed offshore wind turbine and (ii) floating offshore wind turbine. Also, important issues that are being considered as the current challenge in offshore wind farms are the turbine layout and the way electricity is transmitted from the ocean to the shore [55].

Offshore installations currently consist of only a small percentage of the renewable energy market. However, due to the advancement of technology in the design and evaluation of these types of energy resources, it is expected that much progress will be made shortly. Offshore wind farms are in the early stages of their commercialization. They demand a higher cost of capital than onshore wind farms, but this can be compensated by higher capacity factors [56]. Offshore wind farms allow more widespread utilization of wind energy potentials. The reason for the higher capacity factors and the possibility of more use of offshore wind energy are as follows:

- There are no obstacles and restrictions for installing wind turbines for offshore turbines.
- It is possible to build sizeable enormous wind farms offshore.
- In places where the wind speed is average, it can be constructed.
- Offshore turbines have more extended and higher blades, leading to more swept areas and higher electricity outputs.

The offshore turbines are designed for use in offshore. Due to the lack of focus on such issues as shaking and impulse, noise, and visual contamination, there is a relatively different technical path. Although the issue of increasing turbine size for offshore turbines is a problem, this will increase the profit but also increase the operating costs. In this regard, the changing of the design and the ability to consider considerations are likely to provide better conditions in the design of offshore turbines.

Now, new turbines have a power of at least 5 MW. Therefore, a 1000 MW power plant can be achieved by installing 200 turbines [56]. Increase in the cost of the offshore wind turbine installation in the sea and the transfer of energy to the coast are most significant problems which need to be considered. Researchers are still trying to find the ways to reduce the cost of ocean wind farm.

Another challenge in the construction of offshore wind farms is the shortage of large ships that can carry large and heavy parts such as turbines. Also, another challenge in the field of offshore wind farms is the incentive to participate in the electricity market. Power transfer from the plant to the power grid using suitable infrastructures is also challenging for the use of this future energy. There are many other challenges that need to be addressed with the availability of sufficient technology in the world and companies who are active in wind turbine production [57]. Currently, the number of companies specialized in this field is insufficient, and it is expected that the number of these companies will increase shortly. Finally, to expand the use of this energy source, the training of a specialist who can build and

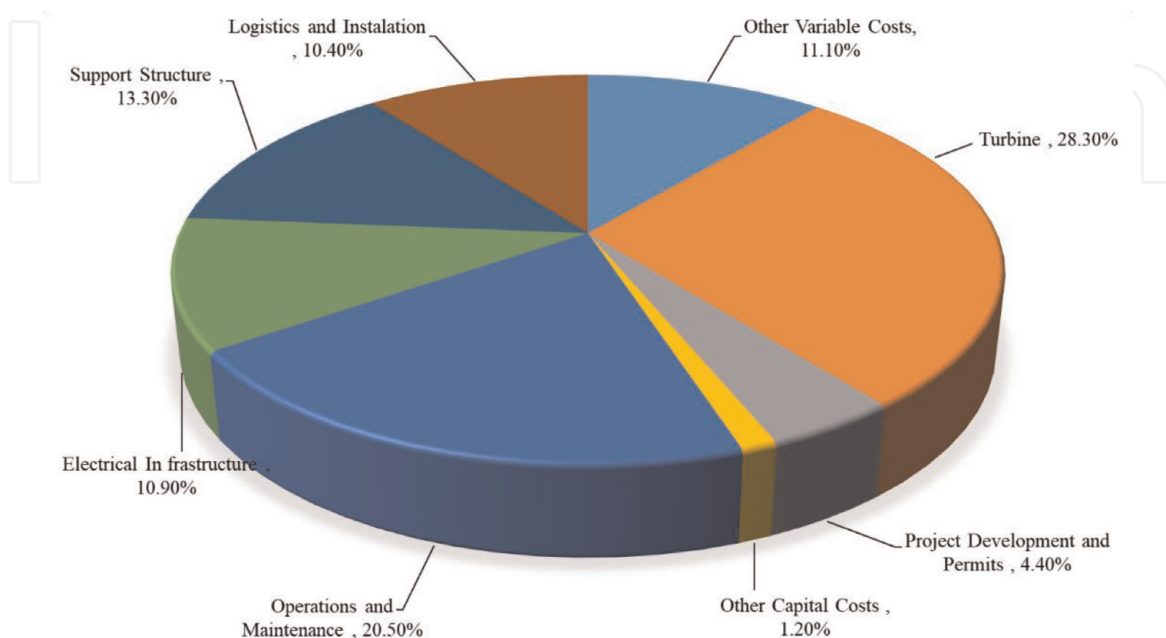


Figure 25.
The lifecycle of an offshore power plant.

operate offshore wind farms is another issue that should be addressed by electricity companies.

Regarding the abovementioned explanation, the major challenges of offshore wind technology are the high cost of offshore wind provision, lack of current infrastructure to support the fabrication such as installation, operation interconnection, maintenance of the system, and the challenges related to the lack of site data and lack of experience.

Figure 25 shows the lifecycle of an offshore power plant. According to this diagram, to solve the first challenge, it should be possible to reduce the impact of this problem in the long-term reports, with the development of industries and the reduction of installation costs and increased reliability of the system.

Nowadays, installation of ocean wind turbines requires specialized vessels, grid interconnections, purpose-built portside infrastructure, and robust undersea electricity transmission lines will be useful from the financial point of view. Regarding the last challenge, ocean wind projects confront new and untested allowing processes, which contributes to the uncertainty and risk faced by potential project developers and financiers.

Author details

Foad H. Gandoman^{1,2}, Abdollah Ahmadi³, Shady H.E. Abdel Aleem^{4*},
Masoud Ardehshiri⁵, Ali Esmaeel Nezhad⁶, Joeri Van Mierlo^{1,2} and
Maitane Berecibar^{1,2}

1 Research Group MOBI—Mobility, Logistics, and Automotive Technology
Research Center, Vrije Universiteit Brussel, Brussels, Belgium

2 Flanders Make, Heverlee, Belgium

3 School of Electrical Engineering and Telecommunications, The University of New
South Wales, Sydney, NSW, Australia

4 Mathematical, Physical and Engineering Sciences, 15th of May Higher Institute of
Engineering, Cairo, Egypt

5 Department of Electrical Engineering, Kazerun Branch, Islamic Azad University,
Kazerun, Iran

6 Department of Electrical, Electronic, and Information Engineering, University of
Bologna, Italy

*Address all correspondence to: engyshady@ieee.org

IntechOpen

© 2020 The Author(s). Licensee IntechOpen. Distributed under the terms of the Creative Commons Attribution - NonCommercial 4.0 License (<https://creativecommons.org/licenses/by-nc/4.0/>), which permits use, distribution and reproduction for non-commercial purposes, provided the original is properly cited. 

References

- [1] Blaabjerg F, Ma K. Wind energy systems. *Proceedings of the IEEE*. 2017; **105**(11):2116-2131
- [2] Lua X, McElroya MB, Kiviluomac J. Global potential for wind-generated electricity. *PNAS*. 2009; **106**(27): 10933-10938
- [3] Lua X, McElroya MB. Chapter 4—Global potential for wind-generated electricity. In: *Wind Energy Engineering A Handbook for Onshore and Offshore Wind Turbines*. Elsevier; 2017. pp. 51-73
- [4] Zheng CW, Li CY, Pan J, Liu MY, Xia LL. An overview of global ocean wind energy resource evaluations. *Renewable and Sustainable Energy Reviews*. 2016; **53**:1240-1251
- [5] Li W, Yao H, Wang H, Wang Z. Research progresses in assessment of China's offshore wind energy resources. *Journal of Renewable and Sustainable Energy*. 2014; **6**(05):31-38
- [6] GWEC-Global-Wind-2015-Report_April-2016_22_04, www.gwec.net
- [7] Leary D, Esteban M. Recent developments in offshore renewable energy in the Asia-Pacific region. *Ocean Development & International Law*. 2011; **42**:94-119
- [8] Makridis C. Offshore wind power resource availability and prospects: A global approach. *Environmental Science & Policy*. 2014; **6**(05):31-38
- [9] Mytilinou V, Kolios AJ, Di Lorenzo G. A comparative multi-disciplinary policy review in wind energy developments in Europe. *International Journal of Sustainable Energy*. 2015; **36**(8):754-774
- [10] The European offshore wind industry. *Key Trends and Statistics 2016*. windeurope.org
- [11] Belward A, Bisselink B, Bódis K, Brink A, Dallemand J-F, de Roo A, et al. *Renewable energies in Africa*. Luxembourg: Publications Office of the European Union; 2011. Available from: <http://www.jrc.ec.europa.eu/>
- [12] Musial W, Heimiller D, Beiter P, Scott G, Draxl C. 2016 Offshore Wind Energy Resource Assessment for the United States. NREL, Denver West Parkway: National Renewable Energy Laboratory; 2016
- [13] Daniel J, Liu S, Pan J. Potential impacts and economic value of US offshore wind. In: *IEEE Power & Energy Society General Meeting*; Denver, CO. 2015. pp. 1-5
- [14] Sun X, Huang D, Wu G. The current state of offshore wind energy technology development. *Energy*. 2012; **41**(1):298-312
- [15] Li W, Zhou H, Liu H, Lin Y, Xu Q. Review on the blade design technologies of tidal current turbine. *Renewable and Sustainable Energy Reviews*. 2016; **63**: 414-422
- [16] Nejad AR, Guo Y, Gao Z, Moan T. Development of a 5 MW reference gearbox for offshore wind turbines. *Wind Energy*. 2016; **19**:1089-1106
- [17] Toftevaag T. Specialization Course ELK 12. NTNU; 2012
- [18] Blaabjerg F, Ma K. Future on power electronics for wind turbine systems. *IEEE Journal of Emerging and Selected Topics in Power Electronics*. 2013; **1**(3): 139-152
- [19] Gandoman FH, Sharaf AM, Abdel Aleem SHE, Jurado F. Distributed FACTS stabilization scheme for efficient utilization of distributed wind energy systems. *International Transactions*

- on Electrical Energy Systems. 2017; 27(11):1-20
- [20] Gandoman FH, Ahmadi A, Sharaf AM, Siano P, Pou J, Hredzak B, et al. Review of FACTS technologies and applications for power quality in smart grids with renewable energy systems. *Renewable and Sustainable Energy Reviews*. 2018;82:502-514
- [21] El-mohr I. Renewable energy systems. *Wind Energy*. 2010. Available from: <http://slideplayer.com/slide/10266678/>
- [22] Bhutto DK, Ansari JA, Chachar F, Katyara S, Soomro J. Selection of optimal controller for active and reactive power control of doubly fed induction generator (DFIG). In: *Computing, Mathematics and Engineering Technologies (iCoMET), 2018 International Conference on*. IEEE; 2018. pp. 1-5
- [23] Wu C, Nian H, Pang B, Cheng P. Adaptive repetitive control of DFIG-DC system considering stator frequency variation. *IEEE Transactions on Power Electronics*. 2018;34(3):3302-3312
- [24] Sáiz-Marín E, Lobato E, Egidio I. New challenges to wind energy voltage control. Survey of recent practice and literature review. *IET Renewable Power Generation*. 2017;12(3):267-278
- [25] Parida A, Chatterjee D. Integrated DFIG-SCIG-based wind energy conversion system equipped with improved power generation capability. *IET Generation, Transmission & Distribution*. 2017;11(15):3791-3800
- [26] Lin F-J, Tan K-H, Tsai C-H. Improved differential evolution-based Elman neural network controller for squirrel-cage induction generator system. *IET Renewable Power Generation*. 2016;10(7):988-1001
- [27] Wang Y, Meng J, Zhang X, Xu L. Control of PMSG-based wind turbines for system inertial response and power oscillation damping. *IEEE Transactions on Sustainable Energy*. 2015;6(2): 565-574
- [28] Hu J, Nian H, Hu B, He Y, Zhu Z. Direct active and reactive power regulation of DFIG using sliding-mode control approach. *IEEE Transactions on Energy Conversion*. 2010;25(4): 1028-1039
- [29] Naidu NS, Singh B. Grid-interfaced DFIG-based variable speed wind energy conversion system with power smoothening. *IEEE Transactions on Sustainable Energy*. 2017;8(1):51-58
- [30] Kouadria S, Messlem Y, Berkouk EM. Sliding mode control of the active and reactive power of DFIG for variable-speed wind energy conversion system. In: *Renewable and Sustainable Energy Conference (IRSEC), 2015 3rd International*. Marrakech, Morocco: IEEE; 2015. pp. 1-8
- [31] Ranga KP, Sukumar GD, Pakkiraiah B, Rao MS. Neuro fuzzy based P s & Q S controller for Doubly Fed Induction Generator with wind turbine. In: *Electrical Power and Energy Systems (ICEPES), International Conference on*. Bhopal, India: IEEE; 2016. pp. 139-144
- [32] Mohanty A, Patra S, Ray PK. Robust fuzzy-sliding mode based UPFC controller for transient stability analysis in autonomous wind-diesel-PV hybrid system. *IET Generation, Transmission & Distribution*. 2016;10(5):1248-1257
- [33] Hamane B, Doumbia M, Bouhamida M, Benghanem M. Control of wind turbine based on DFIG using Fuzzy-PI and Sliding Mode controllers. In: *Ecological Vehicles and Renewable Energies (EVER), 2014 Ninth International Conference on*. Monte-Carlo, Monaco: IEEE; 2014. pp. 1-8

- [34] Li P, Wang J, Wu F, Li H. Nonlinear controller based on state feedback linearization for series-compensated DFIG-based wind power plants to mitigate sub-synchronous control interaction. *International Transactions on Electrical Energy Systems*. 2018;**29**: e2682
- [35] Taher SA, Dehghani Arani Z, Rahimi M, Shahidehpour M. A new approach using combination of sliding mode control and feedback linearization for enhancing fault ride through capability of DFIG-based WT. *International Transactions on Electrical Energy Systems*. 2018;**28**:e2613
- [36] Ashouri-Zadeh A, Toulabi M, Bahrami S, Ranjbar AM. Modification of DFIG's active power control loop for speed control enhancement and inertial frequency response. *IEEE Transactions on Sustainable Energy*. 2017;**8**(4): 1772-1782
- [37] Ghosh S, Kamalasan S. An integrated dynamic modeling and adaptive controller approach for flywheel augmented DFIG based wind system. *IEEE Transactions on Power Systems*. 2017;**32**(3):2161-2171
- [38] Mendel JM, Wu D. Critique of “a new look at Type-2 fuzzy sets and Type-2 fuzzy logic systems”. *IEEE Transactions on Fuzzy Systems*. 2017;**25**(3):725-727
- [39] Raju SK, Pillai G. Design and implementation of type-2 fuzzy logic controller for DFIG-based wind energy systems in distribution networks. *IEEE Transactions on Sustainable Energy*. 2016;**7**(1):345-353
- [40] Yassin HM, Hanafy HH, Hallouda MM. Enhancement low-voltage ride through capability of permanent magnet synchronous generator-based wind turbines using interval type-2 fuzzy control. *IET Renewable Power Generation*. 2016;**10**(3):339-348
- [41] Khooban MH, Niknam T, Sha-Sadeghi M. Speed control of electrical vehicles: A time-varying proportional-integral controller-based type-2 fuzzy logic. *IET Science, Measurement & Technology*. 2016;**10**(3):185-192
- [42] Sarabakha A, Fu C, Kayacan E, Kumbasar T. Type-2 fuzzy logic controllers made even simpler: From design to deployment for UAVs. *IEEE Transactions on Industrial Electronics*. 2018;**65**(6):5069-5077
- [43] Chaoui H, Khayamy M, Aljarboua AA. Adaptive interval type-2 fuzzy logic control for PMSM drives with a modified reference frame. *IEEE Transactions on Industrial Electronics*. 2017;**64**(5):3786-3797
- [44] Rahman NHA, Zobaa AF. Integrated mutation strategy with modified binary PSO algorithm for optimal PMUs placement. *IEEE Transactions on Industrial Informatics*. 2017;**13**(6):3124-3133
- [45] Wei L-X, Li X, Fan R, Sun H, Hu Z-Y. A hybrid multiobjective particle swarm optimization algorithm based on R2 indicator. *IEEE Access*. 2018;**6**:14710-14721
- [46] Mahdi FP, Vasant P, Abdullah-Al-Wadud M, Watada J, Kallimani V. A quantum-inspired particle swarm optimization approach for environmental/economic power dispatch problem using cubic criterion function. *International Transactions on Electrical Energy Systems*. 2018;**28**(3):e2497
- [47] Serrano FE, Flores MA. C++ library for fuzzy type-2 controller design with particle swarm optimization tuning. In: *Central American and Panama Convention (CONCAPAN XXXV)*, 2015 IEEE Thirty Fifth. Tegucigalpa, Honduras: IEEE; 2015. pp. 1-7
- [48] Wang D, Ma N, Wei M, Liu Y. Parameters tuning of power system

stabilizer PSS4B using hybrid particle swarm optimization algorithm. *International Transactions on Electrical Energy Systems*. 2018;**28**:e2598

[49] Hurel J, Mandow A, García-Cerezo A. Tuning a fuzzy controller by particle swarm optimization for an active suspension system. In: *IECON 2012-38th Annual Conference on IEEE Industrial Electronics Society*. Montreal, QC, Canada: IEEE; 2012. pp. 2524-2529

[50] Lee JH, Song J-Y, Kim D-W, Kim J-W, Kim Y-J, Jung S-Y. Particle swarm optimization algorithm with intelligent particle number control for optimal design of electric machines. *IEEE Transactions on Industrial Electronics*. 2018;**65**(2):1791-1798

[51] Koad RB, Zobaa AF, El-Shahat A. A novel MPPT algorithm based on particle swarm optimization for photovoltaic systems. *IEEE Transactions on Sustainable Energy*. 2017;**8**(2):468-476

[52] Tulay G, İskender İ, Erdem H. Optimal tuning of a boost PFC converter PI controller using heuristic optimization methods. *International Transactions on Electrical Energy Systems*. 2017;**27**(12):e2458

[53] Javadi MS, Esmaeel Nezhad A. Intelligent particle swarm optimization augmented with chaotic searching technique to integrate distant energy resources. *International Transactions on Electrical Energy Systems*. 2017;**27**(12): e2447

[54] Ahmed SS. Finite element modeling of large diameter monopiles in dense sand for offshore wind turbine foundation. In: *Proceedings of the ASME 2015 34th International Conference on Ocean, Offshore and Arctic Engineering*, May 31–June 5, 2015, Newfoundland, Canada

[55] Malhotra S. “Design and Construction Considerations for

Offshore Wind Turbine Foundations”, Research and Innovations. New York: P D Network; 2004

[56] Oh KY, Nam W, Ryu MS, Kim J, Epureanu BI. A review of foundations of offshore wind energy convertors: Current status and future perspectives. *Renewable and Sustainable Energy Reviews*. 2018;**88**:16-36

[57] Santos AC, Perez JP, Diez DB, Rodríguez C. Offshore wind energy: A review of the current status, challenges and future development in Spain. *Renewable and Sustainable Energy Reviews*. 2016;**64**:1-18